CLLAMM RESEARCH CENTRE | GOYDER INSTITUTE FOR WATER RESEARCH

Modelling climate change scenarios and their impact on microalgae communities in the Coorong

March 2026

Daniel Chilton, Justin Brookes, Matt Hipsey and Sophie Leterme

The CLLMM Research Centre has the objective of developing and delivering locally driven, innovative, and impactful research that reflects community and First Nations priorities to provide an evidence base to address critical needs of the CLLMM region. The CLLMM Research Centre will also bring together our First Nations, local community and scientists to create and share knowledge, and support our well-informed and engaged community and empower our future generations to be part of the solution.

The Goyder Institute for Water Research Coorong, Lower Lakes and Murray Mouth (CLLMM) Research Centre, based in Goolwa SA, was established in 2023 through funding by the Australian Government.

Australian Government

Department of Climate Change, Energy, the Environment and Water

The Goyder Institute for Water Research is a partnership between the South Australian Government through the Department for Environment and Water, CSIRO, Flinders University and Adelaide University.

Enquires should be addressed to: CLLMM Research Centre
Level 1, 92 Barrage Road
Goolwa, SA 5214
e-mail: info@cllmmresearchcentre.org

This report may be cited as:

Chilton D, Brookes J, Hipsey M, and Leterme S (2026). *Modelling climate change scenarios and their impact on microalgae communities in the Coorong*. A report prepared for the Goyder Institute for Water Research CLLMM Research Centre, Goolwa, South Australia. https://doi.org/10.25909/33189117.

Disclaimer

This report has been prepared by the Flinders University and reviewed in accordance with the publication protocols of the Goyder Institute for Water Research. The authors confirm that they own, or have permission to use, all visual content, including photographs, charts, and graphs presented in this publication, and that they have the right to publish such content. The report contains independent scientific/technical advice to inform decision-making. The independent findings and recommendations of this report are subject to separate and further consideration and decision-making processes and do not necessarily represent the views of the Australian Government or Goyder Institute for Water Research partner organisations. The Goyder Institute for Water Research and its partner organisations do not warrant or make any representation regarding the use, or results of the use, of the information contained herein about its correctness, accuracy, reliability, currency or otherwise and expressly disclaim all liability or responsibility to any person using the information or advice. Information contained in this document is, to the knowledge of the project partners, correct at the time of writing.

Table of Contents

EXECUTIVE SUMMARY **1**

ACKNOWLEDGEMENTS **4**

1 INTRODUCTION **5**

2 MATERIALS AND METHODS **7**

2.1 PHYTOPLANKTON SAMPLING 8
2.2 WATER QUALITY SAMPLING 9
2.3 OTHER ENVIRONMENTAL DATA 10
2.4 DATA ANALYSIS 10
2.4.1 Variable screening 10
2.4.2 Categorisation of flow periods, habitats, phytoplankton taxonomic groups and harmful algae 11
2.4.3 Phytoplankton diversity analyses 13
2.4.4 Comparing resemblance matrices 14
2.4.5 Analysis of phytoplankton abundance and diversity as continuous variables 14
2.4.6 Predicting harmful algae abundance 14

3 RESULTS **17**

3.1 CLIMATE PERIODS SHAPE ENVIRONMENTAL CHARACTER AND ASSOCIATED PHYTOPLANKTON COMMUNITIES 17
3.2 ENVIRONMENTAL DRIVERS OF PHYTOPLANKTON COMMUNITIES 25
3.2.1 Correlation analyses 25
3.2.2 Comparing environmental and phytoplankton community resemblance matrices 27
3.2.3 Generalised additive models 29
3.3 PHYTOPLANKTON COMMUNITIES WITHIN SALINITY-DERIVED HABITATS 34
3.4 PREDICTING HARMFUL ALGAE 41

4 DISCUSSION **45**

4.1 FLOW PERIODS SHAPE THE COORONG ECOSYSTEM 45
4.2 ENVIRONMENTAL DRIVERS OF PHYTOPLANKTON COMMUNITY ABUNDANCE AND DIVERSITY 45
4.3 THE EFFECTS OF SALINITY ON THE PHYTOPLANKTON COMMUNITY 47
4.4 THE EFFECTS OF WATER LEVEL ON THE PHYTOPLANKTON COMMUNITY 48
4.5 SALINITY-DERIVED HABITATS PROVIDE A STRONG BASIS FOR CHARACTERISATION OF PHYTOPLANKTON COMMUNITIES 48
4.6 HYDROLOGICAL CHANGE 49
4.7 PHYTOPLANKTON RESPONSE 50
4.8 FOOD WEB CONSEQUENCES 50
4.9 XGBOOST MODEL 51
4.10 HAB RISK 52
4.11 FUTURE WORK 54

5 CONCLUSION **55**

6. REFERENCES **56**

Executive Summary

The Coorong, a Ramsar-listed coastal lagoon of ecological, cultural and economic importance, is undergoing change as a result of climate-driven shifts in freshwater inflows, temperature, sea level and extreme weather events. Phytoplankton are important bioindicators of these changes due to their rapid turnover rates and are foundational to the functioning of the Coorong's food web. This report synthesises 16 years of phytoplankton and environmental data (2007–2023) to examine how climate-mediated flow variation shapes the Coorong's microalgal communities, supporting a predictive framework to understand future environmental trajectories and phytoplankton responses under climate change. Through an integrated analysis combining long-term monitoring, statistical modelling, machine learning and habitat-based ecological characterisation, this study delivers a comprehensive assessment of how climate variability affects phytoplankton community dynamics and harmful algal bloom (HAB) risk in the Coorong.

A full range of hydrological conditions were captured in this study, from the Millennium Drought (extreme dry) to a large River Murray flood (extreme wet). These contrasting climate periods produced dramatic shifts in barrage flows, water levels, salinity, temperature and nutrient concentrations, which in turn restructured phytoplankton abundance, diversity and community composition.

The Coorong's environmental conditions significantly differed across flow periods. During the dry and extreme dry periods, freshwater inputs declined lowering water levels and increasing salinity to levels exceeding 190 PSU in the South Lagoon. Wet and extreme wet periods reversed these conditions, producing rapid freshening, increased hydrological flushing that removed nutrients and salt from the system and increased water levels, that further diluted salt and nutrients. Phytoplankton communities demonstrated strong, statistically significant responses to these changes, with significantly lower abundances under both extreme wet and dry conditions, but higher richness under wetter conditions and higher evenness during drought.

Across an ensemble of analytical approaches, including multiple correlation analysis, ordination, distance-based linear modelling and generalised additive models, salinity and water level emerged as the dominant drivers of phytoplankton abundance, diversity and community structure. These variables are tightly coupled and both controlled by freshwater inflows. Higher water levels and lower salinities promoted Cyanobacteria and Chlorophyte abundance. Conversely, increasing salinity altered species composition across all taxonomic groups, with increasing dominance of Diatoms and Dinoflagellates. Other important secondary drivers of phytoplankton community dynamics included temperature, distance from the Murray Mouth (representing hydrodynamic and salinity gradients) and nutrient concentrations (particularly NO_X and PO_4), although their influence was weaker and more variable across statistical models.

To characterise responses to hydrological change, phytoplankton communities were classified into six salinity-derived habitats spanning freshwater (H1) to extreme hypersalinity (H6). Community composition, abundance and diversity significantly differed between habitats. Key patterns included:

- Freshwater and low-brackish habitats (H1–H2) had the highest richness but lower evenness, driven by Cyanobacteria and Chlorophyte dominance, particularly under wetter periods. However, H2 demonstrated the most equal representation of all taxonomic groups,
- High-brackish to marine conditions (H3) displayed moderate diversity and high evenness and were dominated by Diatoms and Dinoflagellates,
- Hypersaline habitats (H4–H5) supported very high picophytoplankton abundance and Diatom dominance, and
- Extreme hypersaline conditions (H6) had the lowest richness but highest evenness and were dominated by Diatoms and Dinoflagellates with limited representation from other groups.

These habitat-based community descriptions provide a strong foundation for forecasting future ecological states using hydrological model outputs that predict salinity.

A total of 106 potentially harmful algal bloom forming species (HABs) were identified across the study period, including 82 toxin-producing species. Most HABs occurred in low-salinity habitats (H1–H2) in the North Lagoon, especially during the post-drought wet period in 2012. Although HAB events were generally infrequent and short-lived, two notable bloom events occurred:

1. A Cyanobacteria bloom from January to June 2012 in the North Lagoon consisting of multiple species, though dominated by *Aphanocapsa* sp. and exceeding medium to high risk thresholds, and
2. A Dinoflagellate bloom during the extreme dry period, where *Alexandrium* spp. reached action-level abundances across all sampling sites.

Despite overall low HAB prevalence, the action-level abundances of *Alexandrium* species capable of producing toxins warrants ongoing vigilance, particularly under future climate scenarios that may increase the frequency and intensity of low-flow, high-salinity conditions or sharp nutrient pulses.

An extreme gradient boost (XGBoost) machine learning model was used to predict HAB species abundance from environmental variables. The model performed strongly across much of the dataset, explaining 77% of the variation in HAB abundance, with a normalised root mean square error of 5.7%. The model's predictive performance declined under very high observed HAB abundances (> 1.0 x 10^8 cells L^{-1}), suggesting that extreme bloom events are harder to predict due to their rarity and non-linear ecological triggers. SHapley Additive exPlanations (SHAP) values were used to quantify each environmental predictor variable's contribution to the variation explained by the model. Salinity was revealed as the most influential predictor, aligning with results from other analyses, with higher salinity strongly suppressing HAB formation. pH was the

second most important variable, exerting mostly negative effects on HAB abundance. NO_X and distance from the Murray Mouth were moderate predictors linked to nutrient supply and spatial-chemical gradients, with NO_X exerting a positive influence on HAB formation, while HAB abundance declined with distance from Murray Mouth. The XGBoost model was developed as a tool to better understand the broad context of harmful algal proliferation in the Coorong, but not to be used as a primary method for risk assessment. However, this model has the potential to be further developed to predict the abundances of individual species that have defined cell count risk thresholds and pose a significant threat to the Coorong.

Climate change projections for the Coorong predict continued declines in freshwater inflows, increased air and water temperatures, higher variability in droughts and floods and increasing marine influence with sea-level rise. Under future conditions, the Coorong is expected to experience more frequent and prolonged hypersalinity, particularly in the South Lagoon, resulting in a decline in low-salinity habitats (H1–H2) that currently support higher species richness and Cyanobacteria and Chlorophyte diversity and abundance. Picophytoplankton, Diatoms and Dinoflagellate abundances are predicted to increase, with decreasing species richness as hypersaline habitats (H4–H6) expand. Reducing species richness and the decline of several taxonomic groups will impact the food web, affecting trophic transfer efficiency. Increasing picophytoplankton dominance will increase turbidity, reducing submerged macrophyte habitat with further consequences for the Coorong's biodiversity. Increasing frequency and intensity of drought increases the vulnerability of the Coorong to toxin-producing Dinoflagellate HABs. Without sufficient freshwater inflows, the system risks declining to a permanent degraded state that resembles the end of the Millennium Drought (2007–2010).

To maintain a healthy phytoplankton community and Coorong ecosystem, the following recommendations are outlined:

1. Maintain and enhance freshwater flows to preserve low-salinity habitats critical for phytoplankton diversity, HAB mitigation and hydrological flushing to limit picophytoplankton dominance and maintain water clarity,
2. Implement regular and continuing phytoplankton monitoring to track changes in phytoplankton communities across varying flow periods, detect early HAB signals and improve predictive modelling of phytoplankton dynamics. It is recommended that this monitoring includes testing algal-produced toxin levels,
3. Incorporate phytoplankton community responses to coupled hydrodynamic–biogeochemical-ecological models predicting salinity, water level, temperature and nutrient inputs to capture the spatiotemporal dynamics of the Coorong,
4. Refine machine learning models predicting HABs by further refining model hyperparameters and incorporating additional variables and species-specific predictors to improve bloom detection, particularly under extreme abundances,
5. Investigate species interactions and grazing dynamics, including co-occurrence networks, which strongly influence phytoplankton community composition, an
6. Strengthen HAB risk frameworks by developing species-specific thresholds for the Coorong and integrating outputs into management response protocols.

Acknowledgements

We acknowledge the cultural connections to the land and connected waters, as well as the cultural significance of waterbirds that exist between people of the Ngarrindjeri and Boandik Nations across the Coorong, Lower Lakes, and Murray Mouth region. We recognise that First Nations peoples' spiritual, social, cultural, and economic practices come from their lands and waters, and they continue to maintain their cultural heritage, economies, languages, and laws which are of ongoing importance. We are committed to fostering and nurturing ongoing relationships with First Nations communities in the CLLMM region as we collectively work toward healthy, resilient and thriving lands, waters, ecosystems and communities across the region.

This project was funded by the Goyder Institute for Water Research's CLLMM Research Centre, which is funded by the Australian Government. We thank the CLLMM Research Centre staff for project initiation, support and management. We thank the Goyder Institute for Water Research, Research Advisory Committee and two anonymous reviewers for constructive feedback on the report.

The authors acknowledge additional funding support for the data collection in this project from the Australian Research Council's Discovery Project funding scheme (DP0666420 and DP110101679) and the South Australian Government's Healthy Coorong, Healthy Basin Program (2019–2022), which was jointly funded by the Australian and South Australian governments. We also acknowledge support from the ARC Training Centre for Biofilm Research and Innovation (IC220100003). The authors would like to acknowledge the Department for Environment and Water (DEW) for giving access to the Coorong National Park and SA Water for access across the barrages.

The authors wish to thank the following people who provided support in collecting and processing samples: AD Roozbehani, S Komar, E Tuuri, S Brooke, W Drummond, J Maillard, SA Pinki, N Rogers, T Jamieson, M Waycott, E Bevan, M Couraudon-Réale, N Navong, A Smith, A Van der Beek, D Jardine, J Young, S Brett, J Jendyk, D Hemraj and E Abs.

1 Introduction

Climate conditions shape shallow aquatic ecosystems by mediating environmental conditions and structuring biological communities (Jeppesen et al., 2021). For example, climate affects hydrological conditions and water budgets, such as water circulation and retention, by influencing freshwater and tidal inputs and evaporation rates (Huang et al., 2020). Climate also affects water temperature, highly influencing life histories and primary, secondary and tertiary production (Bonacina et al., 2023; Yvon-Durocher et al., 2010). Anthropogenic climate change is modifying these systems through abrupt changes due to rising sea levels, increasing temperatures, modified flow regimes and increasing extreme events such as floods and droughts (Chilton et al., 2021; Huang et al., 2020). These changes can be enhanced by anthropogenic actions, such as vegetation clearance, land use change, dam construction and water diversion, which further modify environmental conditions (Chilton et al., 2021; Priya et al., 2023).

Shallow coastal lagoons are important aquatic ecosystems, with high productivity and biodiversity that provide a wide range of ecosystem services including storm surge buffering, fisheries, amenity and cultural value, nutrient cycling and retention and carbon sequestration (de Wit et al., 2020; Garrido et al., 2011; Keneally et al., 2025). These shallow lagoons are oriented parallel to the coast but are separated from the ocean by a barrier with one or more inlets (Fairbridge, 1980). They are distributed globally on every continent and make up 13% of the Earth's coastline (Kjerfve, 1994). Despite their global importance, these lagoons suffer from frequent disturbances and are often highly ecologically degraded (de Wit et al., 2020; Singh et al., 2022). This is due to their location at the interface between river-catchments and the sea, making them vulnerable to climate change and direct anthropogenic stressors from both realms (Huang et al., 2020; Stein et al., 2021). Climate and direct anthropogenic stressors are modifying the ecological structure and function of shallow coastal lagoons, resulting in eutrophication and salinisation (Keneally et al., 2024; Mosley et al., 2023; Priestley et al., 2022).

The salinity gradient is a key feature structuring biological communities in coastal lagoons (Chilton et al., 2021; Keneally et al., 2025), with salinity considered a master variable controlling the distribution and abundance of taxa (Lee and Kuhn, 2019), driven by physiological tolerances of organisms (Velasco et al., 2018). Many organisms have life history traits adapted to varying salinity, which can cue fish spawning (Brookes et al., 2022) and sexual or asexual reproduction in submerged macrophytes (Kim et al., 2013). Phytoplankton community structure is strongly affected by salinity, with varying abundance, diversity and distribution of taxa forming along the salinity gradient (Li et al., 2021; Sun et al., 2022; Tunca et al., 2024).

At the base of aquatic food webs, phytoplankton are important primary producers that provide food resources to higher trophic organisms (Balzano et al., 2015; Garcia-Oliva and Wirtz, 2025), including zooplankton, bivalves, crustaceans and fish (Lancelot and Muylaert, 2011). They are essential for nutrient cycling, carbon storage and oxygen production that is vital to the health of aquatic organisms (Singh et al., 2022).

Their short life cycles make them highly responsive to environmental change, serving as powerful bioindicators of coastal lagoon health (Chandel et al., 2023). However, modifications in environmental conditions, such as increasing water temperature, salinsation and eutrophication can promote the proliferation of some phytoplankton species, resulting in harmful algal blooms (HABs) (Derot et al., 2020; Jöhnk et al., 2008). Associated with these blooms are adverse water quality conditions, the death of aquatic and terrestrial organisms and a serious human health risk, as several species produce toxins that harm the liver, nervous system and gastrointestinal tract (Jöhnk et al., 2008; Pinto et al., 2023). In addition, when the bloom crashes, widespread hypoxic and anoxic conditions occur due to heightened microbial decomposition of the dead phytoplankton material, causing suffocation of aquatic biota (Burdick et al., 2020; Hoagland et al., 2002). Due to both the importance and risk phytoplankton species pose, it is important to understand the impacts of climate change on ecosystem function and phytoplankton community dynamics in shallow coastal lagoons.

Despite their global distribution and ecological significance, shallow coastal lagoons are poorly studied in comparison to other aquatic systems (Keneally et al., 2025), with limited information on the drivers of phytoplankton community dynamics in these systems (D'Alelio et al., 2022; Singh et al., 2022). This restricts our ability to predict phytoplankton species responses to climate change, presenting a challenge for managers to promote lagoon ecosystem health and mitigate severe negative consequences of HABs.

This study examined how changing climate conditions modified the environmental conditions and phytoplankton community in the Coorong, a Ramsar-listed shallow coastal lagoon of local and international importance, facilitating predictions of the phytoplankton community under future conceptual ecosystem states. This was achieved by: 1) examining the responses of environmental conditions and phytoplankton community structure and abundance to changing climate conditions, 2) determining the principal environmental drivers of change in phytoplankton community abundance and diversity, and 3) characterising the phytoplankton community under varying salinity-derived habitat states. By coupling delineations of phytoplankton communities within salinity-derived habitats to the proportions of these habitats under varying climate conditions, our study predicts the phytoplankton composition under future states of the Coorong ecosystem.

2 Materials and Methods

The Coorong, together with the Lower Lakes and Murray Mouth (CLLMM) was recognised as a Wetland of International Importance under the Ramsar Convention on Wetlands in 1985 for its role in providing a wide range of habitat types and housing exceptional biological diversity (Kingsford et al., 2011). The Coorong supports commercial fisheries, tourism and recreational activities such as boating, fishing and bird watching (Sitters, 2018). The Coorong is also highly significant in cultural value for the Ngarrindjeri traditional owners (Hemming et al., 2018).

Sampling for the Coorong's phytoplankton community and water quality was conducted at 20 locations spanning ~100 km along the length of the Coorong, from the fresh to brackish waters near the Murray Mouth to hypersaline waters near Salt Creek (Figure 1). Sampling was conducted 46 times sporadically between February 2007 and April 2023, however, not all sites were visited during each sampling trip and large gaps between sampling occurred, including a 6-year gap between October 2014 and October 2020 (see Table 1 for details).

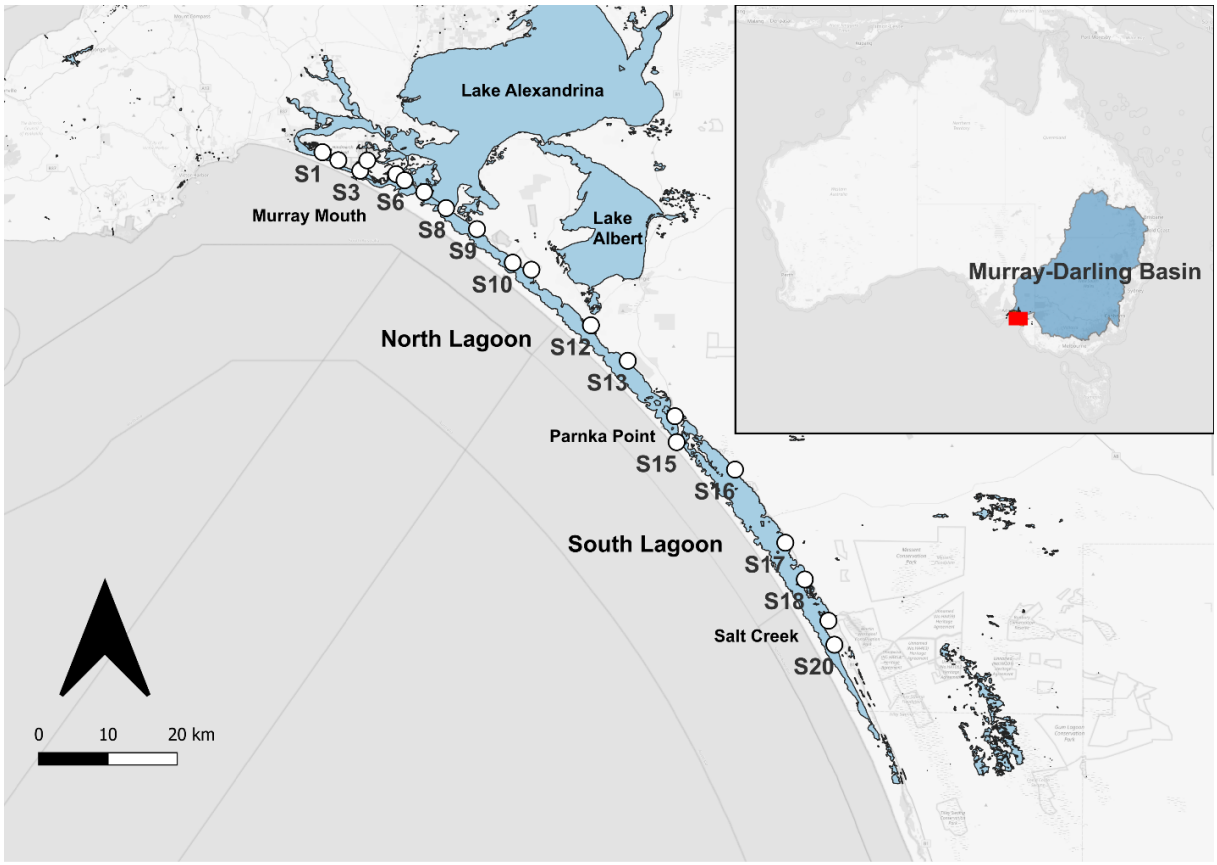

Figure 1. The Coorong, Lower Lakes (Lake Alexandrina and Lake Albert) and Murray mouth (CLLMM) indicated in light blue. Sampling sites are denoted by the white circles. The inset map denotes the location of the CLLMM (red square) within the Australian continental context with the Murray-Darling Basin denoted by the dark blue. The large continuous grey shaded areas in the main and inset maps denote the ocean.

Table 1. Sampling campaigns throughout the 2007–2023 sampling period. For each sampling campaign, the month-year and the sites are given.

SAMPLING CAMPAIGN	MONTH-YEAR	CLIMATE CONDITIONS	NO. SITES	SITES
1	February 2007	Extreme dry (drought)	20	S1–20
2	May 2009	Extreme dry (drought)	20	S1–20
3–8	August 2011–January 2012	Wet (post-drought)	5	S3, S10, S13, S18–19
9	February 2012	Wet (post-drought)	17	S1–6, S10–18, S20
10–11	March–April 2012	Wet (post-drought)	5	S3, S10, S13, S18–19
12	May 2012	Wet (post-drought)	13	S1–3, S9, S11–18, S20
13–14	June–July 2012	Wet (post-drought)	5	S3, S10, S13, S18–19
15	August 2012	Wet (post-drought)	18	S1–9, S11–18, S20
16–17	September–October 2012	Wet (post-drought)	6	S3, S10, S13–14, S18–19
18	November 2012	Wet (post-drought)	13	S1–4, S9–13, S15–17, S20
19–23	December 2012–April 2013	Wet and intermediate (post-drought)	6	S3, S10, S13–14, S18–19
24	May 2013	Intermediate (post-drought)	17	S2–14, S16–18, S20
25–26	June–July 2013	Intermediate (post-drought)	5	S3, S10, S13, S18–19
27	August 2013	Intermediate (post-drought)	18	S1–9, S11–18, S20
28–39	November 2013–October 2014	Intermediate (post-drought)	7	S1, S5, S9, S12, S14, S17, S20
40–43	October 2020, December 2020, March 2021, June 2021	Dry (pre-flood)	5	S12–14, S18–19
44–46	November 2022, January 2023, April 2023	Extreme wet (flood)	5	S3, S10, S12, S14, S19

2.1 Phytoplankton sampling

At each sampling site, triplicate water samples (500 mL) were collected 30 cm below the water's surface for enumerating phytoplankton species abundances. The water samples were fixed with Lugol's iodine (5% final concentration) to preserve the structure of the organisms' chloroplast and subsequently identified and enumerated by Microalgal Services (Ormond, Victoria). Samples were filtered through mixed cellulose ester membranes (5 mm pore size; Sterlitech, Kent, USA). The phytoplankton cells on the filters were resuspended in a smaller volume of filtrate from the same sample. One millilitre of this suspension was then pipetted into a Sedgewick Rafter and counted using a Zeiss Axiolab upright microscope equipped with bright-field and phase contrast optics (Carl Zeiss Microscopy, Thornwood, USA). Cells were identified

to the genus, or species, level based on their key taxonomic features (Hallegraeff et al., 2010).

Picophytoplankton data captured during the drought (2007–2009) were measured by flow cytometry following methods outlined in Balzano et al. (2015). Flow cytometry is often used to enumerate picophytoplankton abundance because these cells are very small (typically < 2 µm in size) and can be difficult to detect or reliably distinguish using traditional microscopy, whereas flow cytometry enables rapid detection and quantification of such small, low-signal cells (Marie et al., 1997). At the time of the drought sampling, it was considered best practice to only use flow cytometry to measure picophytoplankton abundance. However, flow cytometry can underestimate picophytoplankton abundance relative to direct microscopic counts, due to detection limits and difficulties in consistently identifying all cells (Salmi et al., 2021). For this reason, microscopic enumeration of picophytoplankton was implemented from 2011 onwards, as it provides directly comparable measures of abundance across all phytoplankton size classes. From each sampling site, 1 mL of water was fixed with 2% paraformaldehyde (ProSciTech, Thuringowa, Australia) prior to flash freezing in liquid nitrogen and storage at 80 °C until further analysis. Picophytoplankton cells were enumerated from the samples based on pigment autofluorescence. The samples were incubated at 80 °C for 10 min and fluorescent marker beads (1 mL, Molecular probes, Eugene, USA) were added to all samples as an internal size and concentration standard prior to analyses which were performed using a FacsCanto flow cytometer (Becton Dickinson, San José, USA). For each sample forward-angle light scatter, side-angle light scatter (SSC), SYBR I Green (530 nm), red (670 nm), and orange (585 nm) fluorescence were recorded. Picophytoplankton were discriminated based on SSC, as well as on natural orange (phycoerythrin) and red (chlorophyll) fluorescence, as described by Marie et al. (1997). After each flow cytometry analysis, the concentration of marker beads was estimated by epifluorescence microscopy and used to normalize the abundance of all picophytoplankton populations.

2.2 *Water quality sampling*

Water quality measurements and water sample collection for nutrients were performed 30 cm below the water's surface. A TPS 90FL-T multi-parameter probe (TPS Pty Ltd, Brisbane, Australia), measured temperature (°C), pH, salinity (Practical Salinity Units, PSU), turbidity (Nephelometric Turbidity Unit, NTU) and dissolved oxygen concentrations (%SAT) were recorded. Dissolved inorganic nutrient concentrations (i.e., silica [Si], ammonia [NH_3], orthophosphate [PO_4] and nitrate/nitrite [NO_X]) were determined using a San++ Segmented Flow Analyser (SFA; Skalar Inc., Breda, The Netherlands) following published methods (Hansen and Koroleff, 1999). For the analysis, 100 mL of water was filtered in triplicate through bonnet syringe Minisart filters (0.45 mm pore size, Sartorius Stedim, Dandenong, Australia) to remove large particles. Filtrates were then stored at -20 °C until analysis. Prior to analysis, the samples were thawed and mixed before injecting approximately 3 mL of each sample into the SFA.

2.3 Other environmental data

Water level, flow over the barrages and complementary water quality data were retrieved from the South Australian Department for Environment and Water <https://water.data.sa.gov.au/Data/Map/Parameter/NoParameter/Location/Type/Interval/Latest> (DEW, 2025). Water level and barrage flow data were averaged per month. Total monthly rainfall data recorded at Meningie, South Australia, were retrieved from BOM (2025) <https://www.bom.gov.au/location/australia/south-australia/upper-south-east/bsa_pt074-meningie>.

2.4 Data analysis

2.4.1 Variable screening

All variables in the dataset were screened for missing data and collinearity prior to being included in statistical analyses. Environmental variables were screened for collinearity by performing: 1) Spearman-rank correlations between all combinations of variables and 2) variance inflation factor (VIF) testing (Dormann et al., 2013). VIF testing was undertaken by performing multiple regression analysis predicting total phytoplankton community and picophytoplankton abundances, Margalef's richness and Pielou's evenness using all environmental variables in the model, with VIF scores computed for each variable in the model. Significant collinearity was deemed to occur when the Spearman $\rho \geq 0.8$ and/or the VIF score ≥ 5 (Dormann et al., 2013).

Spearman-rank correlations were also performed between all environmental variables and phytoplankton abundance and diversity to explore relationships between environmental conditions and phytoplankton community assemblages. Spearman-rank correlations were performed in R statistical software (v4.4.3) (R Core Team, 2022).

Picophytoplankton abundance strongly correlated with total phytoplankton community abundance ($\rho = 0.99$; $p < 0.01$). As such, total community abundance was analysed without picophytoplankton, with picophytoplankton abundance being analysed separately. Phytoplankton diversity indices (Margalef's richness and Pielou's evenness) were computed without picophytoplankton as these cells (dia. < 6 µm) were not determined to species level, only the abundance of all picophytoplankton cells were aggregated.

Due to the different methods of picophytoplankton abundance measurements between drought and non-drought samples, a comparison was made between the flow cytometry and Sedgewick Rafter methods from a period where both methods were used in conjunction (from 2011–2014) to highlight variation in cell counts between the two methods. Flow cytometry data were strongly and significantly correlated to Sedgewick Rafter cell count data ($R2 = 0.88$; $p < 0.01$) but tended to underestimate picophytoplankton abundance by an order of magnitude. As such, flow cytometry picophytoplankton abundances ($pico_{flow}$) were corrected by linear regression (equation 1):

$$pico_{corrected} = 0.73\, pico_{flow} + 7.81 \quad (1)$$

The dataset included the following 16 environmental variables: barrage flow, dissolved oxygen (DO), distance from Murray Mouth, Ewe Island water level, NH_3, NO_X, N:P ratio, Parnka Point water level, pH, PO_4, rainfall, salinity, Si, water temperature, turbidity and wind stress. The proportion of missing data was computed for each variable. Barrage flows, distance from Murray Mouth, pH, rainfall, temperature and water level had no missing data, while missing data for salinity and nutrients was quite low (<1%) and these data were gathered from openly available Government of South Australia data (DEW, 2025) that aligned with the time and location of samples collected during this study. Wind stress, Si and turbidity had 47.5%, 47.3% and 36.3% missing data respectively that could not be gathered from additional sources. These were deemed too large to interpolate and were removed from the analyses. DO was also removed as it had considerable missing data (11.53%) and was a confounding variable by being strongly influenced by phytoplankton production in the shallow oxygenated waters of the Coorong (Mosley et al., 2023).

2.4.2 Categorisation of flow periods, habitats, phytoplankton taxonomic groups and harmful algae

The 16-year span of the phytoplankton and environmental dataset captured a wide range of flow conditions, from extreme dry (e.g., drought) to extreme wet (e.g., flood). To determine the influence of freshwater flow on the Coorong ecosystem, the dataset was classified into five distinct flow periods (years data captured) enabling statistical testing and analysis, these being: 1) Extreme dry (2007 and 2009), 2) Dry (2020–2021), 3) Intermediate (2013–2014), 4) Wet (2011–2012) and 5) Extreme wet (2022–2023). In addition, the datasets were also categorised into salinity-derived habitats, whereby habitat 1 is freshwater (H1; <5 PSU), habitat 2 is brackish (H2; 5–20 PSU), habitat 3 is high-brackish to marine (H3; 21–40 PSU), habitat 4 is hypersaline (H4; 41–84 PSU), habitat 5 is high hypersaline (H5; 85–119 PSU) and habitat 6 is extreme hypersaline (H6; ≥120 PSU). These habitats represent the gradient of salinity that characterises the Coorong ecosystem and phytoplankton communities within, as salinity is widely recognised as an important determinant of phytoplankton species diversity, abundance and community composition in the Coorong (Aldridge and Brookes, 2011; Jendyk et al., 2014; Leterme et al., 2015; Schapira et al., 2010).

Phytoplankton species or species groups (e.g., Gymnodinioids < 20 µm) were classified into one of the following taxonomic groups: Chlorophytes, Chrysophytes, Cryptophytes, Cyanoprokaryotes, Diatoms, Dinoflagellates, Euglenophytes, Prasinophytes and Prymnesiophytes. The remaining species which did not fall into one of these groups and were too few to be classified into another group (e.g., one species per group) were grouped together as other phytoplankton.

Phytoplankton species were also classified according to their harmful status. Harmful algal bloom forming species (HABs) were identified based on listings provided by Ahyong et al., (2026), Hallegraeff et al., (2021) and Lundholm et al., (2009 onwards). HABs are characterised by the rapid and excessive accumulation of phytoplankton species that cause harm by producing biotoxins (toxic HABs) or by causing dissolved oxygen depletion, severe shading or physical harm to organisms (non-toxic HABs;

Wurtsbaugh et al., 2019). The primary risk associated with HABs for the Coorong relates to declines in ecosystem health due to mortality of aquatic biota, which can disrupt food web functioning and reduce biodiversity (Giatas et al., 2018). For example, declines in invertebrate communities such as polychaete worms and estuarine snails can affect higher trophic level consumers, including fish and migratory shorebirds (Giatas et al., 2018; Paton et al., 2015). These ecological impacts may, in turn, affect commercial and recreational fisheries, tourism and the broader amenity of the region for local residents.

HAB risk in this study was interpreted primarily using species-specific risk thresholds where available (Table 2), which provide a more direct indication of potential ecological or health impacts. However, species specific risk thresholds from cell counts have not been defined for most harmful algae species observed in our dataset, with risk thresholds only defined for several Cyanobacteria and Dinoflagellate species (Table 2). As such, aggregated harmful algae abundances were used in a broad context to understand the general patterns in potential risk from harmful algae in the Coorong. This was deemed pertinent given that harmful algae species have been very little reported on in the literature to date (e.g., Jamieson et al., 2022). Our study reports the general severity of harmful algae based on exposure level thresholds outlined by the Australian Government National Health and Medical Research Council Guidelines for Managing Risks in Recreational Water (NHMRC 2008) and consist of the following cell counts, following a global review on toxin exposure (Stewart et al., 2006):

- Low < 5,000,000 cells L^{-1}
- Medium 5,000,000–100,000,000 cells L^{-1}
- High > 100,000,000 cells L^{-1}

Stewart et al., (2006) found that individuals exposed to waters of high HAB concentrations were more likely to report symptoms after exposure than those exposed to waters with low HAB concentrations.

Table 2. Specific warning levels for cyanobacteria and dinoflagellate species observed in this dataset.

TAXONOMIC GROUP	SPECIES	SURVEILLANCE LEVEL	ALERT LEVEL	ACTION LEVEL	REFERENCE
Cyanobacteria	*Lyngbya majuscula*	-	≥ 1 cell L^{-1}	Visible scums present	Environmental Health Directorate (2022)
	Microcystis aeruginosa	≥ 500,000 cells L^{-1}	≥ 5,000,000 cells L^{-1}	≥ 50,000,000 cells L^{-1}	NHMRC (2008)
	Trichodesmium spp.	-	≥ 5,000,000 cells L^{-1}	≥ 50,000,000 cells L^{-1}	Environmental Health Directorate (2022)
Dinoflagellates	*Alexandrium* spp.	-	≥ 1,000 cells L^{-1}	≥ 10,000 cells L^{-1}	Environmental Health Directorate (2022)
	Gymnodinium catenatum	-	≥ 10,000 cells L^{-1}	≥ 100,000 cells L^{-1}	Hallegraeff et al., (1995)
	Karenia spp.	-	≥ 50,000 cells L^{-1}	≥ 100,000 cells L^{-1}	Environmental Health Directorate (2022)

2.4.3 Phytoplankton diversity analyses

The total number of species, Margalef's species richness, Pielou's evenness and the Shannon diversity index were performed in PRIMER+ (v7). Margalef's richness index (*d*) was used in the analyses instead of the total number of species as it corrects for the increasing number of species collected with greater numbers of organisms sampled (Death, 2008). It achieves this by dividing the species count by the natural logarithm of the number of sampled organisms (equation 2):

$$d = \frac{S-1}{\ln(N)} \quad (2)$$

Where *S* is the total number of species observed and *N* is the total number of individuals in the sample. Pielou's evenness index (*J'*) measures how evenly the number of individuals are distributed among the species. A community is perfectly even if every species is present in equal proportions and uneven if one species dominates the abundance distribution (Herrmann et al., 2022). Pielou's evenness was calculated by equation 3:

$$J' = \frac{H'}{\ln(S)} \quad (3)$$

Where *H'* is the Shannon diversity index, which was calculated by equation 4:

$$H' = -\sum_{i=1}^{S} p_i \ln(p_i) \quad (4)$$

Where p_i is the proportion of the total individuals belonging to the *i*-th species.

2.4.4 Comparing resemblance matrices

Resemblance matrices were produced to deduce the influence of continuous environmental variables and categorical variables (flow period and habitat) on phytoplankton community composition. Phytoplankton abundance and nutrients (NH_3, NO_X, PO_4 and N:P) were natural logarithm + 1 transformed prior to analysis. The environmental dataset was normalised prior to quantifying the dissimilarity between samples using Euclidean distance. The phytoplankton resemblance matrix was generated using the Bray-Curtis index of similarity. Unconstrained ordination using Principal Coordinate Analysis (PCoA) was used to identify the principal components that explained the most variance in the dataset by visualising the similarity and dissimilarity between samples (Anderson and Willis, 2003; Shapouri et al., 2015).

To elicit the environmental drivers of phytoplankton community structure, several methods were used. Firstly, Pearson correlation coefficients (R^2) were calculated between each environmental variable and the first two axes of the principal component ordinations. Secondly, the phytoplankton resemblance matrix was compared to the environmental resemblance matrix using randomised permutation test for relationships between two matrices (RELATE), Biota and environmental matching (BEST) and distance-based linear modelling (DistLM), which was visualised by distance-based redundancy analysis (dbRDA). The significance of the influence of categorical variables (flow period and habitat) on phytoplankton and environmental resemblance matrices were analysed by permutational analysis of variance (PERMANOVA). Results were deemed statistically significant when $p < 0.05$. All analyses mentioned above were performed in PRIMER+ (v7).

2.4.5 Analysis of phytoplankton abundance and diversity as continuous variables

Phytoplankton abundance and diversity (Margalef's richness and Pielou's evenness) were predicted using Generalised Additive Models (GAMs) in R (v4.4.3; R Core Team, 2022) using package "mgcv" (Pedersen et al., 2019), with variable importance assessed via the package "gam.hp " (Lai et al., 2024) and model diagnostics generated using package "gratia" (Simpson, 2024). Differences in phytoplankton metrics across flow periods, habitats and lagoons were tested with Kruskal–Wallis H tests in R (v4.4.3), followed by Dunn's post-hoc comparisons with Benjamini–Hochberg correction when significant effects were detected using package "FSA" (Ogle et al., 2025).

2.4.6 Predicting harmful algae abundance

Machine learning models are becoming increasingly valuable tools for predicting biological species abundances from a wide range of environmental predictors. This is due to their ability to handle large and complex datasets that capture non-linear relationships, often a pitfall of existing statistical models (Hu et al., 2024; Zhang et al., 2025). Extreme gradient boosting (XGBoost) is a machine learning model that has been successfully applied to phytoplankton datasets with a high predictive accuracy and robustness to outliers, missing values and collinearity (Xu et al., 2024). In this study,

an XGBoost model was applied to predict total harmful algae abundance from environmental variables using the R package "XGBoost" (Chen and Guestrin, 2016). The dataset was randomly partitioned into training (80%) and testing (20%) datasets, with the training dataset used to fit the XGBoost model with the test dataset used for assessment of predictive accuracy. Predictive accuracy was evaluated by calculating the coefficient of determination (R^2), the mean absolute error (MAE) and the root mean square error (RMSE) following equations 5, 6 and 7 below:

$$R^2 = 1 - \frac{\sum(y_i - \hat{y}_i)^2}{\sum(y_i - \bar{y})^2} \quad (5)$$

$$MAE = \frac{1}{n}\sum_{i=1}^{n}|y_i - \hat{y}_i| \quad (6)$$

$$RMSE = \sqrt{MAE} \quad (7)$$

where y_i are the observed values, $\hat{y}_i$ are the predicted values, $\bar{y}$ is the mean of the observed data and n is the number of samples. To improve model performance and balance bias, variance and overfitting, a range of hyperparameters were tuned (Table 3). In addition, a 5-fold cross-validation was used to identify the optimal number of boosting iterations (nrounds) for the XGBoost model to improve generalisation to unseen data. Seven boosting iterations were identified as the optimal number of rounds for model training based on RMSE values. Shapley Additive exPlanations (SHAP) values were computed to quantify how each predictor variable contributes to the model's predictions, summarising variable importance within the model and revealing how modelled relationships vary along the gradient of each environmental predictor (Lundberg and Lee, 2017). SHAP values were calculated and visualised using R package "shapviz" (Mayer and Stando, 2025). It is important to note that specific abundances in the results derived from the XGBoost model are presented for broad context only and are not used as the primary basis for risk assessment.

Table 3. Hyperparameter tuning values used in the XGBoost model predicting total harmful algae abundance from environmental variables.

HYPERPARAMETER	VALUE/TYPE	DESCRIPTION
Booster	gbtree	Specifies that the model uses tree-based boosting. A common booster for ecological prediction because it captures non-linearities and interactions well.
Objective (Distribution)	Tweedie	The Tweedie distribution is appropriate for abundance or data that are continuous, non-negative, and often zero-inflated. It allows modelling a compound Poisson–Gamma process.
Tweedie variance power	1.2	Controls the variance function. Values between 1 and 2 typically represent semi-continuous data with many zeroes, with 1.2 used to account for overdispersed data with a long right tail.
Evaluation metrics	R^2, RMSE, MAE	MAE captures the average error of the model's predictions, with RMSE identifying the error in the same units as the response variable, making it easily interpretable.
Max depth	6	Controls the maximum depth of each tree to prevent overfitting.
Minimum child weight	3	Minimum sum of instance weights required to create a new leaf of a tree. Used to reduce over-splitting noisy data, whereby a higher value makes the model more conservative.
Gamma	0	Gamma is the minimum loss reduction needed to make a further split in the tree. A value of 0 allows the model to explore all splits.
Learning rate (eta)	0.3	Used to reduce overfitting.
Subsample	0.8	Each tree is trained on 80% of the data to reduce overfitting and improve model stability.
Colsample bytree	0.8	Each tree uses 80% of the predictor variables to account for correlated predictor variables.
Reg lambda	1	Regularisation of lambda (ridge penalty) to reduce sensitivity to noise.
Reg alpha	1	Regularisation of alpha (lasso penalty) encourages sparsity by shrinking weak features toward zero.

3 Results

3.1 Climate periods shape environmental character and associated phytoplankton communities

The Coorong's environmental conditions and phytoplankton community were strongly affected by flow periods as both the environmental and phytoplankton community resemblance matrices significantly differed by flow period (Table 4; $p < 0.01$). Pairwise PERMANOVA tests revealed that environmental conditions and phytoplankton communities were significantly different between all combinations of flow periods (Table 4). The greatest difference in environmental conditions was between the extreme wet and extreme dry periods and the least difference between the wet and intermediate periods. For the phytoplankton community, there were very strong differences between the extreme dry and all other periods and between the dry and extreme wet periods.

Table 4. Results of PERMANOVA tests of environmental and phytoplankton community matrices by climate period. 999 permutations were run to calculate *p*-values. PERMANOVA main test results include degrees of freedom (df), sum of squares (SS), Pseudo-F statistic and *p*-value, while the pairwise tests include the pseudo-*t* statistic and *p*-values.

PERMANOVA TEST RESULTS				
Resemblance matrix	Df	SS	Pseudo-F	*p*-value
Environmental	4	1645	59.74	0.001
Phytoplankton	4	5.6×10^5	89.15	0.001
Environmental Pairwise tests			Pseudo-*t*	*p*-value
Extreme dry-wet			7.89	0.001
Extreme dry-intermediate			7.72	0.001
Extreme dry-dry			7.72	0.001
Extreme dry-extreme wet			11.61	0.001
Wet-intermediate			3.82	0.001
Wet-dry			7.60	0.001
Wet-extreme wet			8.00	0.001
Intermediate-dry			8.10	0.001
Intermediate-extreme wet			10.42	0.001
Dry-extreme wet			7.85	0.001
Phytoplankton Pairwise tests			Pseudo-*t*	*p*-value
Extreme dry-wet			12.17	0.001
Extreme dry-intermediate			13.99	0.001
Extreme dry-dry			12.82	0.001
Extreme dry-extreme wet			10.84	0.001
Wet-intermediate			3.98	0.001
Wet-dry			7.36	0.001
Wet-extreme wet			4.91	0.001
Intermediate-dry			8.33	0.001
Intermediate-extreme wet			5.65	0.001
Dry-extreme wet			8.37	0.001

Analysis of principal components of the phytoplankton community highlight a strong differentiation between the extreme dry and all other periods (axes 1), followed by clear separation between the dry and the extreme wet periods, with considerable overlap between the intermediate and wet periods (axes 2) (Figure 2). These results align well with the results of the PERMANOVA pairwise tests (Table 4).

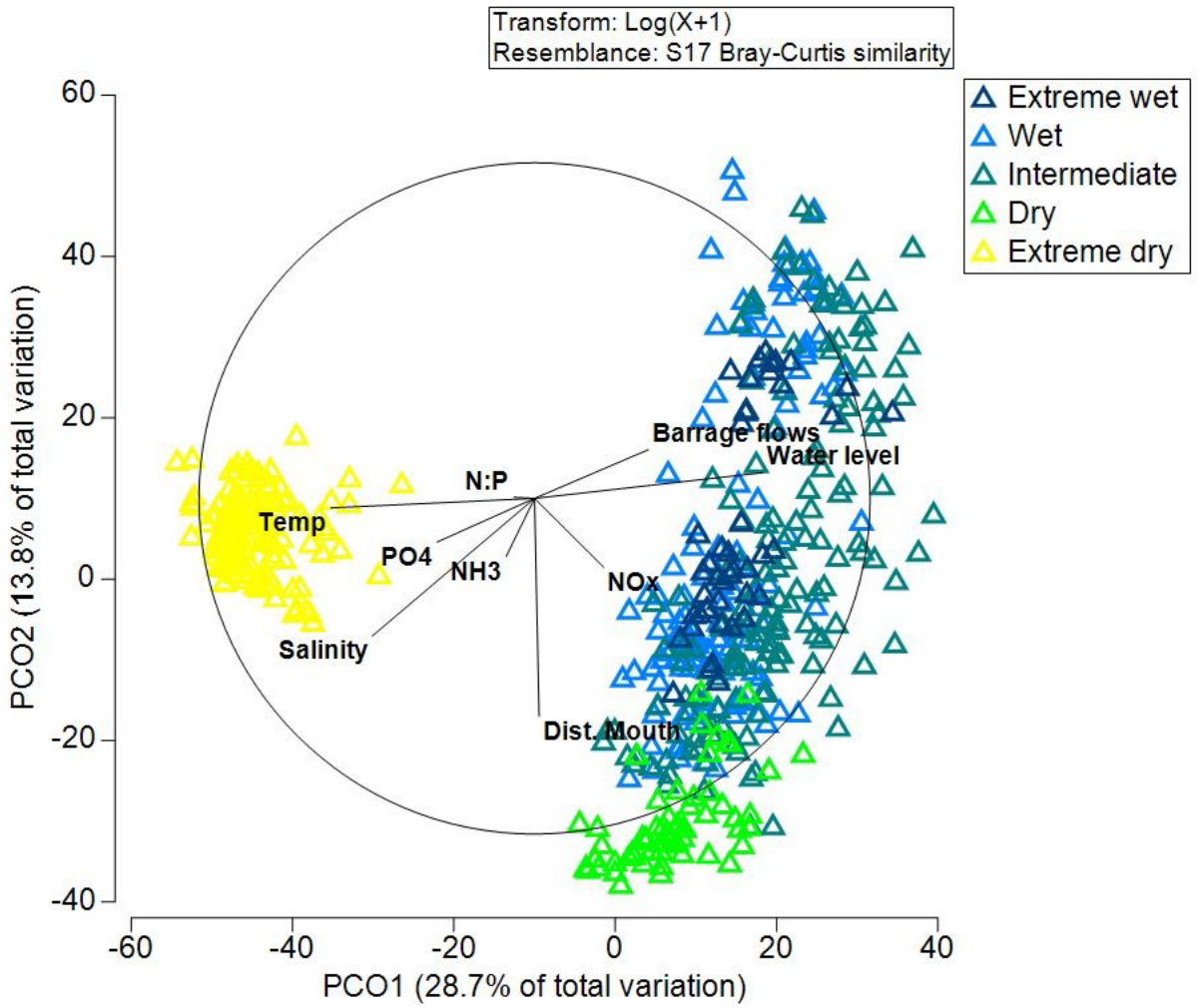

Figure 2. unconstrained ordination of phytoplankton communities coloured by climate period with environmental variables overlayed. unconstrained ordination was performed using principal coordinate analysis (PCoA). Phytoplankton species abundances were natural log +1 transformed prior to generating a resemblance matrix using Bray-Curtis similarity.

All continuous environmental and phytoplankton (total phytoplankton abundance, picophytoplankton abundance, Margalef's richness and Pielou's evenness) variables tested using Kruskal-Wallis H tests significantly differed by climate period (Table 5). Mean month-averaged barrage flow increased with increasingly wet conditions, from 0 GL month^{-1} under extreme dry to 1,856 GL month^{-1} under extreme wet periods, with a concomitant increase in mean water level and decrease in mean salinity. Mean monthly-barrage flow and water level were significantly different between all periods, except between the dry and intermediate periods. Median salinity was significantly greater under extreme dry and dry periods than all others, with salinity peaking at 196

PSU during the Millennium drought. Median salinity was significantly lower during the wet and extreme wet periods than the dry and extreme dry periods. Median temperature was significantly greater during the extreme dry period than all others, in contrast to the intermediate period where median temperature was significantly lower than all other periods. Dissolved nutrients (NH_3, NO_X and PO_4) typically had large variation during all periods, but median values peaked during the extreme wet period, where they were significantly greater than all other periods. N:P ratios were also highly variable with median values significantly greater during the wet and intermediate periods than the others. pH remained alkaline throughout all periods, with the minimum pH value occurring during the intermediate period (8.13). Median pH was significantly greater during the dry and extreme wet periods than all others.

Median phytoplankton and picophytoplankton abundances were significantly greater during the dry period and significantly lower during the extreme dry period than all others by an order of magnitude (Table 5). Median Margalef's richness increased with increasingly wetter conditions, being significantly greater during the extreme wet period than all others and significantly greater in the wet period than the other three. Median Pielou's evenness was significantly greater during the extreme dry period and significantly lower during the dry period than all others.

Table 5. Environmental variables and phytoplankton abundance and diversity by flow periods with Kruskal-Wallis (K-W) H significance tests of each variable by flow period as a factor. Values of the Kruskal-Wallis chi-squared test result are presented with all test results statistically significant ($p < 0.001$). Environmental and phytoplankton values are presented as Mean ± SE (Median; Min–Max).

VARIABLE	UNIT	EXTREME DRY	DRY	INTERMEDIATE	WET	EXTREME WET	K-W TEST CHI-SQ (DF = 4)
Barrage flow	Ave. GL month^{-1}	0 ± 0 (0; 0–0)	113 ± 9.98 (90.5; 33.4–237)	140 ± 11.1 (88.3; 14.9–632)	623 ± 31.7 (503; 186–1131)	1856 ± 161 (1987; 487–3094)	439.6
N:P	-	3.6x10^5 ± 9.5x10^4 (14.5; 0.1–4x10^6)	15.2 ± 1.43 (11.6; 4.4–60.5)	1.1 x10^5 ± 2.6 x10^4 (54.9; 0–1.8x10^6)	898 ± 426 (60.7; 0–4.3x10^4)	13.9 ± 0.94 (12.8; 7.79–33.8)	54.2
NH_3	µM	88.9 ± 12.1 (33.3; 0–500)	32.9 ± 1.33 (30.8; 15–54)	45 ± 6.96 (22.3; 0–875)	159 ± 31.9 (53.1; 0–2676)	77.7 ± 1.9 (78.7; 52.8–99.2)	56.61
NO_X	µM	1.94 ± 0.21 (1.61; 0–10.9)	13.4 ± 2.12 (7.46; 3.02–108)	4.91 ± 0.75 (0.59; 0–46.8)	4.78 ± 0.72 (1.67; 0–46.8)	15.9 ± 0.38 (16.2; 10.7–22.1)	173.35
pH	-	8.42 ± 0.01 (8.42;8.3–8.54)	9.69 ± 0.19 (9.75; 7.56–12.2)	8 ± 0.04 (8.13; 6.08–8.9)	8.13 ± 0.2 (8.17; 7.2–8.68)	9.41 ± 0.07 (9.37; 8.6–10.4)	148.56
PO_4	µM	18.3 ± 3.35 (3.16; 0–168)	3.63 ± 0.21 (3.09; 1.32–8.69)	3.27 ± 0.63 (0.23; 0–36.7)	2.95 ± 0.53 (0.76; 0–32.1)	7.91 ± 0.53 (7.53; 2.53–14.3)	126.52
Salinity	PSU	74.2 ± 4.18 (46.9; 17.7–196)	78.3 ± 3.36 (77.6; 29.6–129)	31.9 ± 1.81 (28.8; 0.46–96)	25.8 ± 2 (14.2; 0.15–73.6)	26.8 ± 3.44 (18; 0.19–69)	166.94
Temperature	°C	24.9 ± 0.3 (25.6; 16.3–30.1)	19.2 ± 0.6 (19.2; 11.7–26.9)	16.6 ± 0.35 (16.6; 2–26.7)	19.3 ± 0.43 (18.9; 10.6–31.9)	19.4 ± 0.42 (18.0; 15.4–25.2)	185.5
Water level	Ave. m AHD month^{-1}	-0.09 ± 0.02 (-0.16; -0.16–0.34)	0.29 ± 0.02 (0.31; 0.07–0.45)	0.36 ± 0.02 (0.38; -0.04–0.77)	0.45 ± 0.02 (0.5; 0.09–0.77)	0.75 ± 0.03 (0.85; 0.46–0.94)	286.95
Phytoplankton abundance (without pico-phytoplankton)	Cells L^{-1}	1.9 x 10^6 ± 1.1 x 10^5 (1.7 x 10^6; 7.9 x 10^4–7.8 x 10^6)	5.7 x 10^7 ± 6.8 x 10^6 (3.3 x 10^7; 4.1 x 10^6–1.7 x 10^8)	2.7 x 10^7 ± 3.7 x 10^6 (1.4 x 10^7; 1.8 x 10^6–4.3 x 10^8)	4.2 x 10^7 ± 7.0 x 10^6 (1.02 x 10^7; 1.0 x 10^6–3.9 x 10^8)	1.9 x 10^7 ± 3.2 x 10^6 (1.15 x 10^7; 4.5 x 10^5–7.6 x 10^7)	261.24
Pico-phytoplankton abundance	Cells L^{-1}	2.5 x 10^7 ± 3.5 x 10^6 (1.8 x 10^7; 1.5 x 10^6–7.3 x 10^7)	2.9 x 10^{10} ± 6.38 x 10^9 (3.72 x 10^9; 1.05 x 10^8–1.75 x 10^{11})	5.9 x 10^9 ± 7.19 x 10^8 (1.95 x 10^9; 1.1 x 10^7–4.9 x 10^{10})	5.89 x 10^9 ± 5.49 x 10^8 (3.7 x 10^9; 1.0 x 10^3–2.95 x 10^{10})	2.28 x 10^8 ± 5.15 x 10^7 (2.1 x 10^7; 1.0 x 10^6–1.0 x 10^9)	319.29

Margalef's richness	-	1.01 ± 0.02 (0.99; 0.42–1.72)	1.06 ± 0.03 (1.02; 0.7–1.87)	1.3 ± 0.03 (1.28; 0.56–2.31)	1.48 ± 0.04 (1.38; 0.68–2.83)	2.64 ± 0.16 (2.29; 1.46–5.29)	210.38
Pielou's evenness	-	0.89 ± 0.003 (0.9; 0.79–0.96)	0.45 ± 0.03 (0.48; 0.16–0.87)	0.63 ± 0.01 (0.68; 0.15–0.88)	0.63 ± 0.02 (0.68; 0.11–0.9)	0.72 ± 0.01 (0.72; 0.41–0.86)	310.69
Harmful algae abundance	Cells L^{-1}	$9.9 \times 10^5 \pm 6.7 \times 10^4$ (9.1×10^5; 3.8×10^4–4.9×10^6)	$3.6 \times 10^6 \pm 5.8 \times 10^5$ (2.8×10^6; 6.6×10^5–2.3×10^7)	$3.9 \times 10^6 \pm 6.2 \times 10^5$ (1.9×10^6; 0–6.9×10^7)	$1.3 \times 10^7 \pm 3.3 \times 10^6$ (1.7×10^6; 0–1.9×10^8)	$6.7 \times 10^6 \pm 1.3 \times 10^6$ (2.8×10^6; 1.4×10^5–3.7×10^7)	84.41

A total of 106 species/species groups were observed in the Coorong between 2007 and 2023 that can potentially cause harm under certain conditions. Of these, 82 were classified as toxic and 24 as non-toxic. The majority of HAB species were Cyanobacteria (43 spp., all toxic), Dinoflagellates (33 spp., 25 toxic) and Diatoms (22 spp., 9 toxic). Other taxonomic groups represented were Raphidophytes with three species and Chlorophytes, Ciliates, Cryptophytes, Prasinophytes and Prymnesiophytes with one species each. The most observed species were *Nitzschia* spp. (Diatoms; 380 occurrences), Gymnodinioid spp. < 20 µm (Dinoflagellates; 354 occurrences), *Gyrodinium* spp. (207 occurrences), *Chrysochromulina* spp. (Prymnesiophytes; 183 occurrences), *Protoperidinium* spp. (Dinoflagellates; 171 occurrences) and *Chaetoceros* spp. (Diatoms; 149 occurrences). The species with the highest observed sample abundances were *Aphanocapsa* sp. (Cyanobacteria; 184,000,000 cells L^{-1}), *Chaetoceros* spp. (67,000,000 cells L^{-1}), *Aphanizomenon gracile* (Cyanobacteria; 50,000,000 cells L^{-1}), *Planktothrix* sp. (filaments; Cyanobacteria; 42,400,000 cells L^{-1}), *Cuspidothrix* sp. (Cyanobacteria; 35,760,000 cells L^{-1}) and *Nitzschia* spp. (26,000,000 cells L^{-1}).

Harmful algae abundance significantly differed by flow period (Table 5). Abundances surpassing the high threshold were observed during the wet period, when flows had returned post Millennium Drought, with low abundances during the extreme dry period that did not surpass the first risk threshold (Figure 3). The spikes in abundance during the wet period consisted primarily of a mix of several Cyanobacteria species: *Aphanocapsa* sp., *Nodularia spumigena*, *Planktothrix* sp. (filaments), *Cuspidothrix* sp., *Merismopedia* sp., *Aphanizomenon* sp. and *A. gracile*. Blooms of these Cyanobacteria occurred from January to June 2012 and were restricted to the northern part of the Coorong between sites S3 (Sugar's Beach, near the Murray Mouth) and S11 (Long Point; Figure 1). Other notable spikes in HAB abundance that surpassed the medium risk level occurred during the intermediate period. The first occurred in March 2013 at S3 and was a bloom of the Diatoms *Chaetoceros* spp. The second spike was an *Aphanocapsa* sp. bloom, which occurred in March 2014 at site S1 (Monument Road, near the Goolwa Barrage). At no other times did the total HAB abundance surpass the medium or high risk levels. The low risk level threshold was surpassed several times in the dry and extreme wet periods. In October 2020 (dry period), a bloom of the Diatoms *Nitzschia* spp. occurred at site S12 (Noonameena). In the extreme wet period, a mixed Cyanobacteria species bloom occurred, consisting of the following species: *Aphanocapsa* sp., *Gomphosphaeria* sp., *Merismopedia* sp., *Woronichinia* sp., *Planktolyngbya* sp. (filaments), *Coelomoron* sp. and cf. *Pseudanabaena* sp. (cells). In November 2022 , the bloom occurred at site S3. In January 2023, it had spread across sites S3 to S12. In April 2023, it had retracted to between S3 and S10 (Mulbin-Yerrok Point).

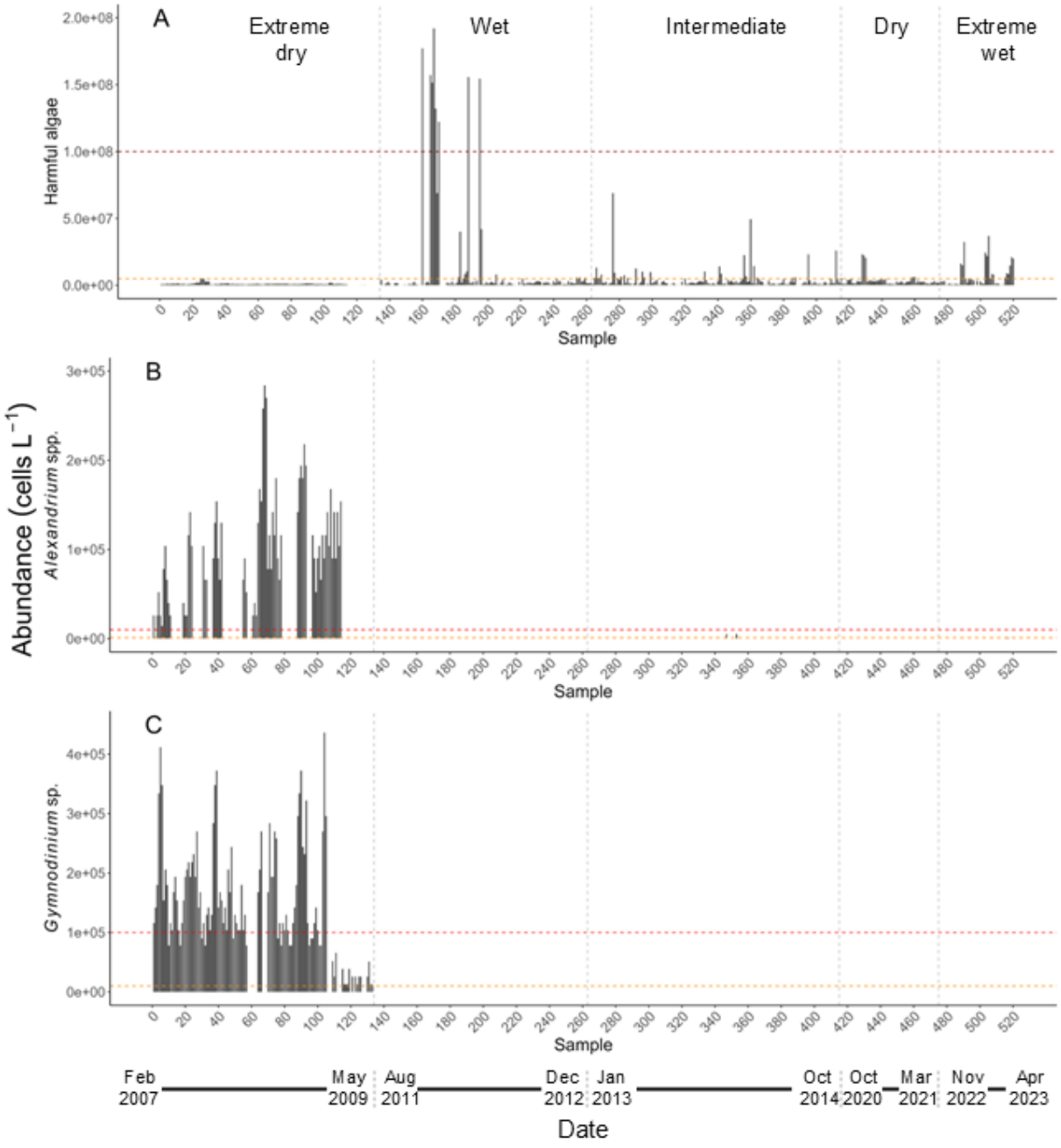

Figure 3. Total Harmful algae abundance (A), *Alexandrium* spp. abundance (B) and *Gymnodinium* sp. abundance (C) by sample over the duration of the sampling period between February 2007 and April 2023. Flow periods are delineated by the vertical dashed grey lines. Dates of each flow period are presented below the sample numbers. Horizontal dashed lines indicate the thresholds of medium (yellow) and high (red) exposure levels outlined by NHMRC (2008) in A and alert (yellow) and action (red) levels outlined in Table 2.

Despite the low total HAB abundances during the extreme dry period, *Alexandrium* abundances were consistently above its respective risk level (Figure 3B). *Alexandrium* spp. were observed 70 times above the action level (≥ 10,000 cells L^{-1}) in February 2007 across all sampling sites (S1–20; Figure 1). After February 2007, *Alexandrium* spp. were only observed six times in the dataset and only three times above the alert level (≥1,000 cells L^{-1}), but never again above the action level (maximum abundance after

February 2007 was 5,000 cells L^{-1}). Five *Alexandrium* species were observed in the dataset, with *A .minutum* being the only species present in February 2007. The remaining *Alexandrium* observations consisted of *A. australiense*, *A. margalefi*, *A. pseudogonyaulax* and *Alexandrium* sp.

Gymnodinium sp. was also consistently observed exceeding the *G. catenatum* risk levels during the extreme dry period, where it was detected 113 times (Figure 3C). Though this *Gymnodinium* species should not be assumed to be of concern as only *G. catenatum* is known to produce toxins that threaten aquatic ecosystem health (Hallegraeff et al., 1995). Like *Alexandrium*, these observations spanned across all sampling sites (S1–20; Figure 1) but were also present in May 2009. *Gymnodinium* sp. was never observed again in the dataset.

In no samples did *Microcystis aeruginosa*, *Trichodesmium* spp. and *Karenia* spp. surpass their respective alert levels (Table 2) with maximum abundances of 47,500, 230,000 and 10,000 cells L^{-1}, respectively. All three species were not observed regularly in the dataset, with 2 observations of *Microcystis aeruginosa*, 5 observations of *Trichodesmium* spp. and 6 observations of *Karenia* spp. Three other *Microcystis* species were observed in the dataset, all with < 5 occurrences and only one (*Microcystis* sp.) surpassing the surveillance level on one occasion with an abundance of 2,500,000 cells L^{-1}. *Lyngbya* sp. was observed once with an abundance of 1 cell L^{-1}, which meets the alert level for *Lyngbya majuscula*, though this *Lyngbya* was not identified to its specific species.

3.2 *Environmental drivers of phytoplankton communities*

3.2.1 Correlation *analyses*

Spearman-rank correlations revealed that the total phytoplankton community and picophytoplankton abundances were significantly correlated with barrage flows, distance from Murray Mouth, NO_x, pH, PO_4, salinity, temperature and water level (Figure 4). Picophytoplankton abundance was also significantly correlated with N:P ratio. Margalef's richness and Pielou's evenness were both significantly correlated to barrage flows, distance from Murray Mouth, NO_x, salinity, temperature and water level, with evenness also significantly correlated with PO_4 and N:P ratio. Distance from Murray Mouth was strongly positively correlated with salinity and NH_3 highlighting a reverse salinity and NH_3 gradient. Salinity was significantly negatively correlated with barrage flows and water level, with water level strongly negatively correlated with temperature.

Water levels at Parnka Point and Ewe Island were highly correlated (Spearman ρ = 0.87; $p < 0.01$), so only Parnka Point water level was used in subsequent analyses (stated as water level hereon). Because water level was also strongly correlated with barrage flow (ρ = 0.82; $p < 0.01$) and rainfall (ρ = 0.87; $p < 0.01$), these two variables were removed from most analyses to avoid redundancy, except where barrage flow was intentionally retained to illustrate its strong influence on the Coorong's environmental conditions and phytoplankton community (Figure 3). The remaining nine environmental variables (distance from Murray Mouth, NH_3, NO_X, N:P ratio, PO_4,

pH, salinity, temperature and water level) displayed no significant multicollinearity (VIF < 5) and were therefore included in all analyses hereon.

Spearman-rank correlation analyses showed that total phytoplankton and picophytoplankton abundances were significantly correlated to multiple environmental factors, including barrage flows, distance from Murray Mouth, NO_X, pH, PO_4, salinity, temperature and water level, with picophytoplankton also significantly correlated to N:P ratio (Figure 4). Margalef's richness and Pielou's evenness were similarly correlated with many of these variables. Distance from the Murray Mouth was positively correlated with salinity and NH_3, indicating the inverse gradient. Salinity was negatively correlated with barrage flows and water level, while water level showed a strong negative relationship with temperature.

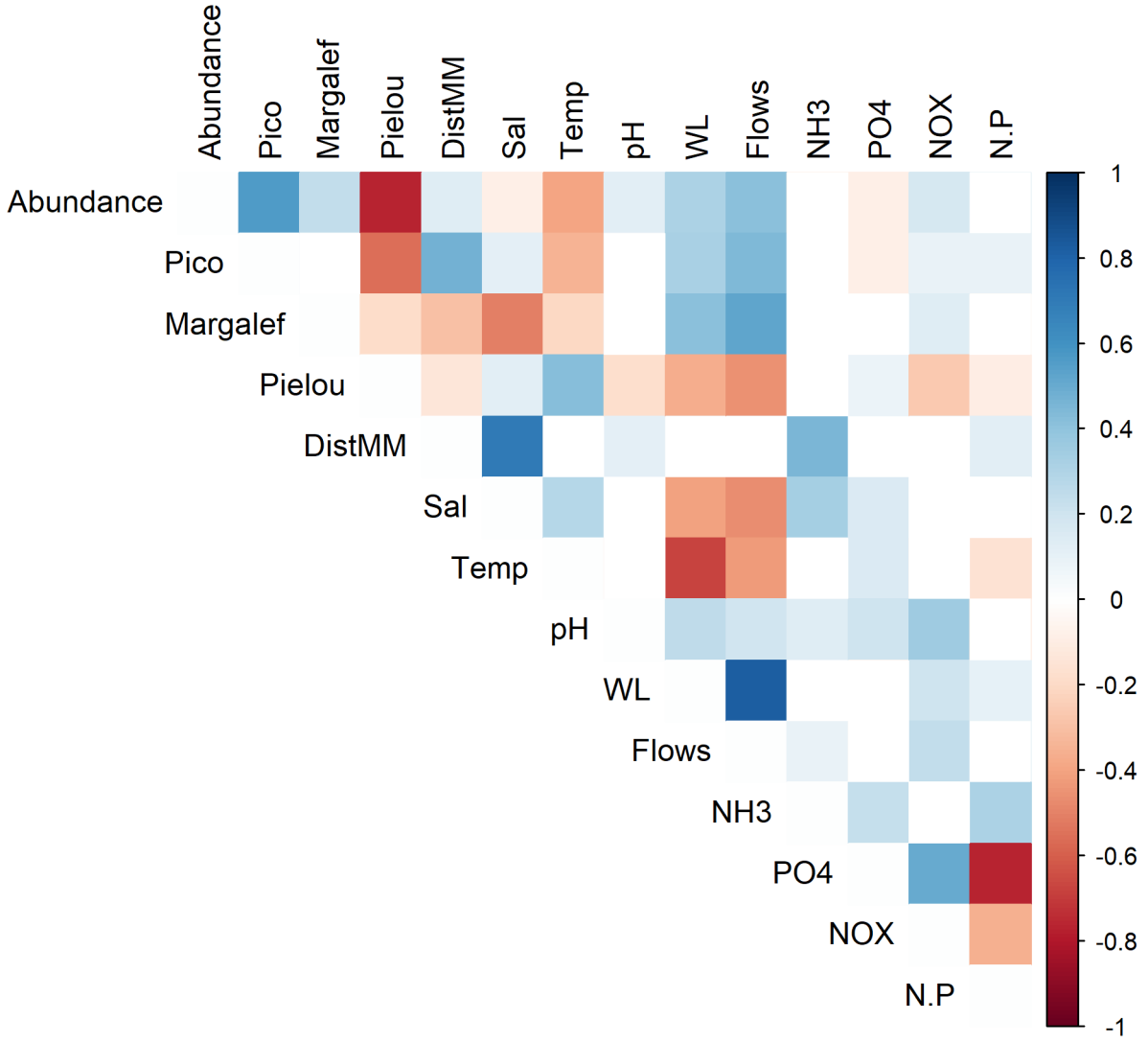

Figure 4. Multiple correlation analysis using Spearman-rank correlations on untransformed phytoplankton (total community abundance, picophytoplankton abundance, Margalef's richness and Pielou's evenness) and environmental variables (distance from Murray Mouth, salinity, temperature, pH, water level, barrage flow, NH3, PO4, NO_X and N:P). Spearman

correlation coefficients (ρ) are displayed as a colour scale from red (negative) to blue (positive) with non-statistically significant correlations ($p > 0.05$) marked as white.

3.2.2 Comparing environmental and phytoplankton community resemblance matrices

The RELATE Spearman rho = 0.26 ($p < 0.01$) demonstrated that the patterns in the environmental data significantly resemble the patterns in the phytoplankton community data with a moderate strength (Table 6). BEST analysis revealed that distance from Murray Mouth, salinity, temperature and water level combined explained the greatest amount of variation in the phytoplankton community (Table 6). For phytoplankton groups, the most common variables produced by BEST were water level (9 groups), salinity (8 groups), temperature (7 groups) and PO_4 (5 groups; Table 6).

Table 6. BEST and RELATE analysis results for total phytoplankton community and for phytoplankton taxonomic groups. BEST variables are listed in alphabetical order. All results statistically significant with *p*-values < 0.01. Statistical significance derived from permutation tests consisting of 999 permutations.

PHYTOPLANKTON GROUPS	RELATE SPEARMAN RHO	BEST VARIABLE(S)	BEST SPEARMAN RHO
Total community	0.26	distance from Murray Mouth, salinity, temperature, water level	0.43
Diatoms	0.12	distance from Murray Mouth, salinity, temperature, water level	0.22
Chlorophytes	0.19	PO_4, salinity, temperature, water level	0.28
Cryptophytes	0.26	N:P ratio, salinity, temperature, water level	0.36
Chrysophytes	0.19	NO_x, PO_4, temperature, water level	0.23
Cyanoprokaryota	0.22	N:P ratio, PO_4, pH, salinity, water level	0.28
Dinoflagellates	0.21	water level	0.34
Euglenophyta	0.13	distance from Murray Mouth, N:P ratio, PO_4, salinity, water level	0.19
Prasinophytes	0.20	PO_4, salinity, temperature, water level	0.31
Prymnesiophyceae	0.1	salinity, temperature, water level	0.17
Other phytoplankton	0.11	N:P ratio, salinity, temperature	0.17

The stepwise DistLM model explained 34.35% of the variation in phytoplankton abundance, with all environmental variables contributing significantly. Water level accounted for the largest share of variation (14.20%), followed by distance from the Murray Mouth (6.44%) and salinity (4.14%). The dbRDA indicated that variation in phytoplankton community structure was primarily driven by a temperature-salinity-water level gradient along axis 1, while axis 2 reflected spatial and chemical gradients

(Figure 5). Temperature (R^2 = 0.75) and salinity (R^2 = 0.58) were strongly positively associated with axis 1, whereas water level (R^2 = -0.85) was strongly negatively associated. Distance from Murray Mouth (R^2 = 0.87), salinity (R^2 = 0.57), pH (R^2 = 0.44) and nutrients (NO_X R^2 = 0.29; NH_3 R^2 = 0.27; PO_4 R^2 = 0.20) were all positively correlated with axis 2. When grouped by salinity-based habitats and lagoon, dbRDA patterns showed axis 1 represents a strong gradient from hypersaline (H6) to freshwater (H1) habitats, and axis 2 reflects the spatial gradient from the North to South Lagoon.

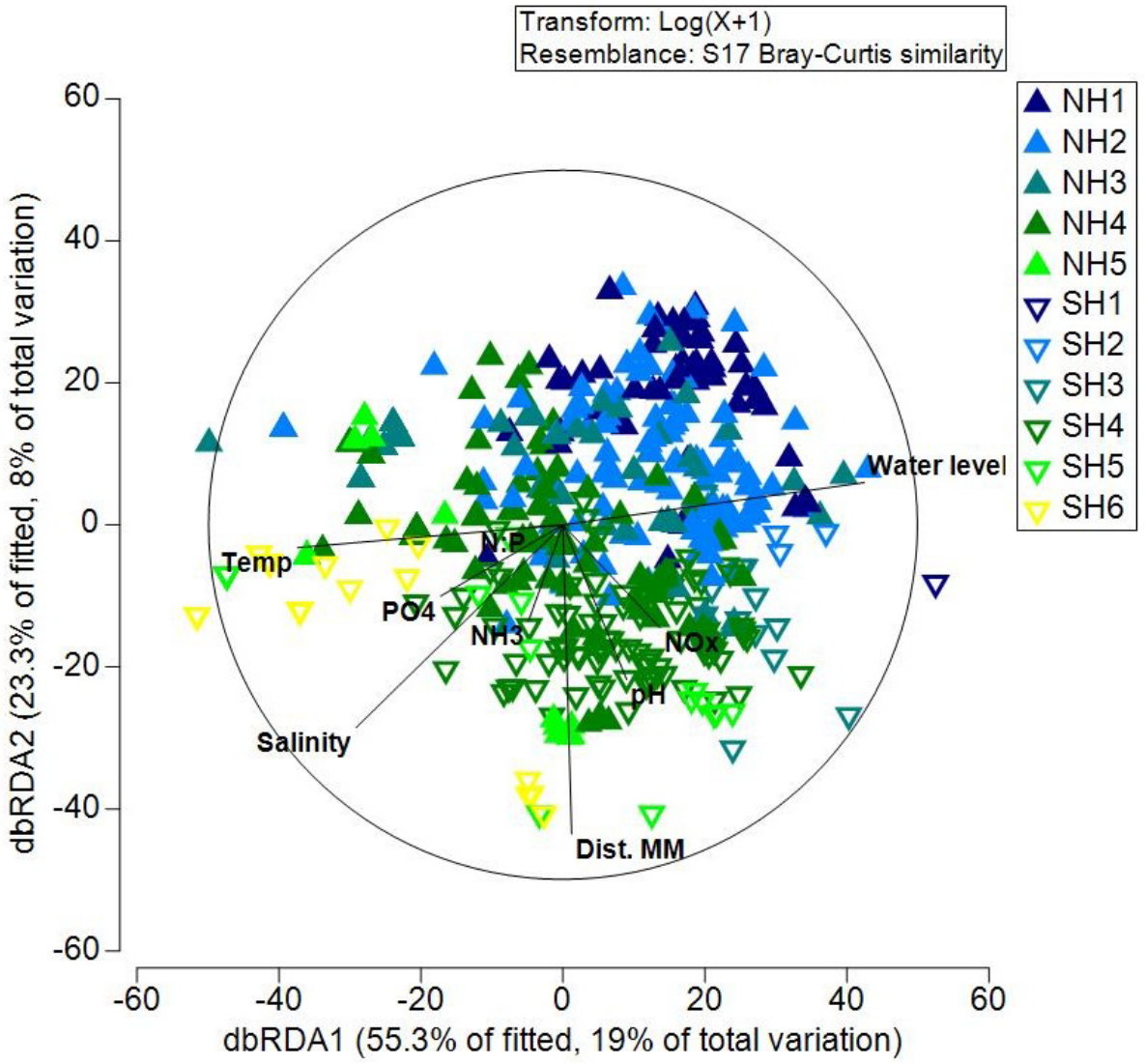

Figure 5. Distance-based redundancy analysis (dbRDA) characterising patterns in phytoplankton community assemblage. The dbRDA was performed including water level, salinity, temperature (temp), distance from Murray Mouth (Dist. MM), pH, PO_4, NH_3, NO_X and N:P ratio. Samples are coloured by salinity-based habitat (H1–H6) with lagoon represented by closed (north, N) and open (south, S) triangles. Phytoplankton abundances were natural log + 1 transformed prior to applying a Bray-Curtis resemblance matrix.

3.2.3 Generalised additive models

Generalised additive models (GAMs) captured non-linear trends when predicting total phytoplankton community abundance (without picophytoplankton), picophytoplankton abundance, Margalef's richness and Pielou's evenness by environmental variables (Figure 6). Distance from Murray Mouth, pH, salinity, temperature and water level were significant in all GAMs, with the significance of nutrients varying between GAMs (Tables 7–10). Salinity and water were consistently the variables that explained the most variation in each GAM with only distance from Murray Mouth explaining slightly more variation than salinity in the GAM predicting picophytoplankton abundance.

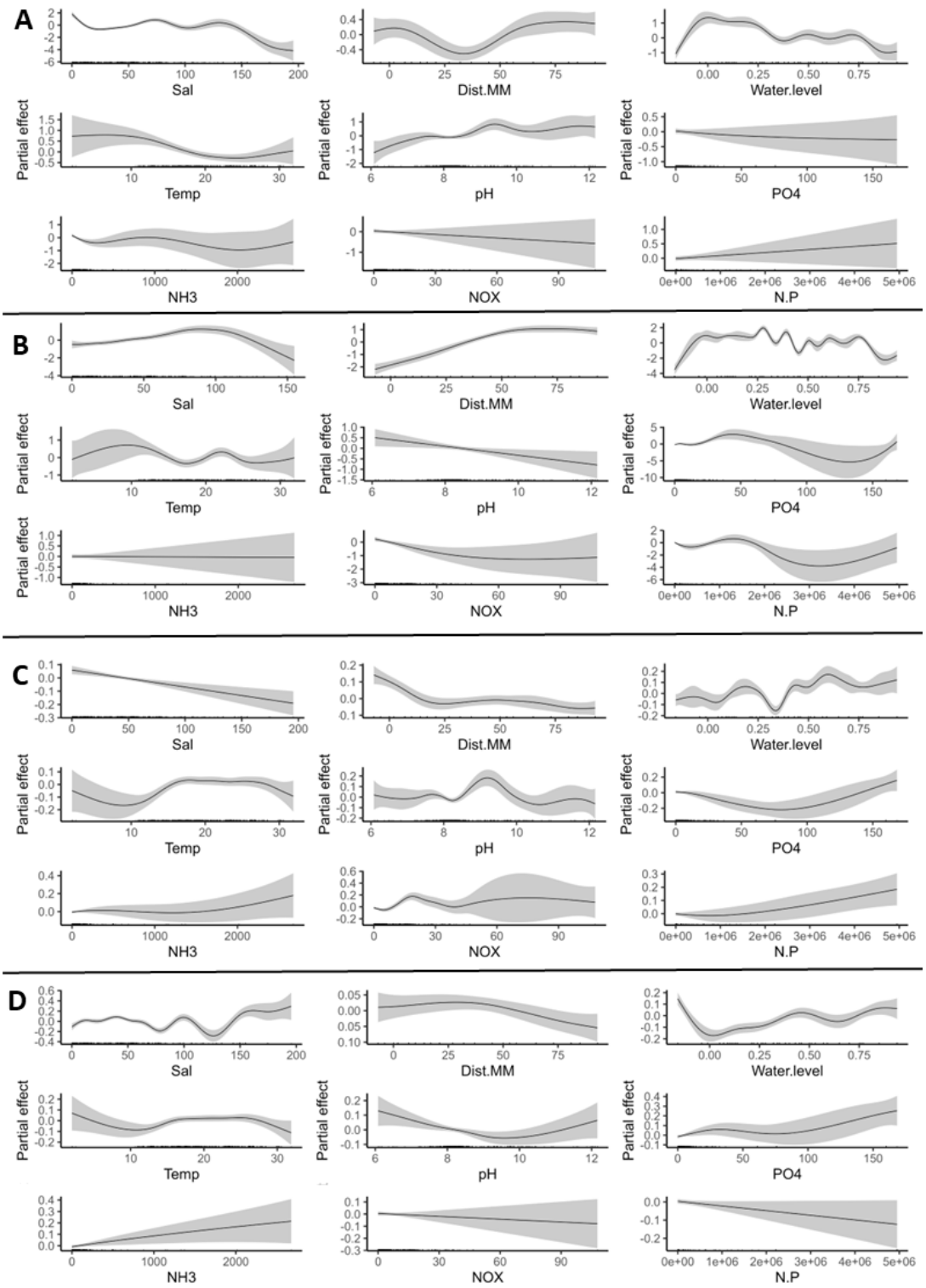

Figure 6. Generalised additive model (GAM) partial effects plots demonstrating the estimated contribution of each predictor variable, whilst holding all other terms at a value of zero contribution, for the GAMs predicting (A) total phytoplankton community abundance (without picophytoplankton), (B) picophytoplankton abundance, (C) Margalef's diversity and (D) Pielou's evenness. Estimated effects of the response variables are centred around zero and displayed at the link scale (y-axes) where positive values indicate an increase in the response while negative values indicate a decrease. Values on x-axes are in the units of the predictor variable displaying how the contribution of each continuous covariate changes across the range of observed values. Uncertainty in estimated contributions are presented by 95% confidence intervals, denoted by the grey shaded area around fitted smooth terms.

Table 7. Generalised additive model (GAM) outputs predicting total phytoplankton community abundance (without picophytoplankton) from nine environmental variables (salinity, distance from Murray Mouth, water level, temperature, pH, PO_4, NH_3, NO_X and N:P ratio).

PHYTOPLANKTON COMMUNITY TOTAL ABUNDANCE (WITHOUT PICOPHYTOPLANKTON) GAM USING A NEGATIVE BINOMIAL DISTRIBUTION WITH LOG LINK				
Model deviance explained	**64.8%**			
Parametric coefficient	**Value**	**SE**	**Z value**	***p*-value**
Intercept	16.33	0.04	414.50	< 0.001
Smooth terms (variables in alphabetical order)		**Effective degrees of freedom**	**Chi-squared**	***p*-value**
Distance from Murray Mouth		5.12	41.05	< 0.001
N:P		1.00	1.38	> 0.05
NH_3		3.81	13.15	< 0.05
NO_X		1.00	0.89	> 0.05
pH		6.32	28.36	< 0.001
PO_4		1.26	0.53	> 0.05
Salinity		8.88	259.71	< 0.001
Temperature		3.65	23.64	< 0.001
Water level		9.56	200.68	< 0.001
Significant variables (in order of % variation explained)		**Deviance explained (%)**		
Salinity		35.92		
Water level		32.74		
Distance from Murray Mouth		6.61		
Temperature		6.33		
pH		5.11		
NH_3		1.11		

Table 8. Generalised additive model (GAM) outputs predicting picophytoplankton abundance from nine environmental variables (salinity, distance from Murray Mouth, water level, temperature, pH, PO_4, NH_3, NO_X and N:P ratio).

PICOPHYTOPLANKTON ABUNDANCE GAM USING TWEEDIE DISTRIBUTION WITH LOG LINK				
Model deviance explained	**79.4%**			
Parametric coefficient	**Value**	**SE**	**Z value**	***p*-value**
Intercept	21.04	0.05	436.30	< 0.001
Smooth terms (variables in alphabetical order)		**Effective degrees of freedom**	**Chi-squared**	***p*-value**
Distance from Murray Mouth		4.12	31.47	< 0.001
N:P		3.00	3.28	< 0.05
NH_3		1.00	0.01	> 0.05
NO_X		2.20	4.73	< 0.01
pH		1.00	6.01	< 0.05
PO_4		6.97	4.28	< 0.001
Salinity		5.56	9.14	< 0.001
Temperature		6.86	3.27	< 0.001
Water level		14.47	23.77	< 0.001
Significant variables (in order of % variation explained)		**Deviance explained (%)**		
Water level		27.66		
Distance from Murray Mouth		23.44		
Salinity		22.43		
PO_4		9.33		
NO_X		4.37		
pH		4.17		
Temperature		4.10		
N:P		1.93		

Table 9. Generalised additive model (GAM) outputs predicting margalef's diversity from nine environmental variables (salinity, distance from Murray Mouth, water level, temperature, pH, PO_4, NH_3, NO_X and N:P ratio).

MARGALEF'S DIVERSITY GAM USING GAMMA DISTRIBUTION WITH SQRT LINK				
Model deviance explained	**73.4%**			
Parametric coefficient	**Value**	**SE**	**T value**	***p*-value**
Intercept	1.15	0.01	205.70	< 0.001
Smooth terms (variables in alphabetical order)		**Effective degrees of freedom**	**F value**	***p*-value**
Distance from Murray Mouth		16.49	3.84	< 0.001
N:P		1.25	6.31	< 0.05
NH_3		1.00	0.80	> 0.05
NO_X		8.43	4.52	< 0.001
pH		8.67	4.26	< 0.001
PO_4		3.10	3.74	< 0.05
Salinity		8.12	4.43	< 0.001
Temperature		24.27	2.35	< 0.001
Water level		17.38	5.05	< 0.001
Significant variables (in order of % variation explained)		**Deviance explained (%)**		
Water level		18.03		
Salinity		14.89		
pH		14.04		
Temperature		13.23		
NO_X		12.35		
Distance from Murray Mouth		12.29		
PO_4		6.14		
N:P		2.91		

Table 10. Generalised additive model (GAM) outputs predicting pielou's evenness diversity from nine environmental variables (salinity, distance from Murray Mouth, water level, temperature, pH, PO_4, NH_3, NO_X and N:P ratio).

PIELOU'S EVENNESS GAM USING BETA DISTRIBUTION WITH LOGIT LINK				
Model deviance explained	**60.4%**			
Parametric coefficient	**Value**	**SE**	**Z value**	***p*-value**
Intercept	0.83	0.03	29.28	< 0.001
Smooth terms (variables in alphabetical order)		**Effective degrees of freedom**	**F value**	***p*-value**
Distance from Murray Mouth		3.46	2.43	< 0.01
N:P		2.90	2.14	< 0.05
NH_3		1.00	5.78	< 0.05
NO_X		1.00	0.003	> 0.05
pH		2.46	2.61	< 0.05
PO_4		2.70	4.79	< 0.001
Salinity		11.09	12.52	< 0.001
Temperature		4.23	2.97	< 0.01
Water level		7.34	12.20	< 0.001
Significant variables (in order of % variation explained)		**Deviance explained (%)**		
Water level		39.00		
Salinity		26.20		
Temperature		12.18		
PO_4		4.91		
Distance from Murray Mouth		4.67		
NH_3		3.69		
pH		2.66		
N:P		0.96		

3.3 *Phytoplankton communities within salinity-derived habitats*

The phytoplankton community resemblance matrix significantly differed by habitat in the PERMANOVA main test (Table 8). In addition, total phytoplankton community abundance, picophytoplankton abundance, Margalef's richness and Pielou's evenness also significantly differed by habitat in Kruskal-Wallis H tests (Table 8). This aligns with the clear separation of phytoplankton communities by habitats in the dbRDA (Figure 5) and supports the framework utilised in this study to predict the Coorong's phytoplankton communities by classification into salinity-derived habitats.

The greatest differences in phytoplankton communities were observed between the lower salinity habitats (H1 and H2) and the high and extreme hypersaline habitats (H5 and H6), as denoted by larger PERMANOVA Pseudo-*t* values. There were also considerable differences between the freshwater-low brackish habitat (H1) and the high brackish-marine and hypersaline habitats (H3 and H4). The hypersaline H4 and H5 habitats were the most similar, having the smallest Pseudo-*t* values of any pairwise test.

Table 11. PERMANOVA and Kruskal-Wallis significance testing of phytoplankton community assemblage, abundance and diversity by habitat. PERMANOVA significance testing conducted on the phytoplankton community resemblance matrix with 999 permutations run to calculate *p*-values. Kruskal-Wallis H tests were conducted on total phytoplankton community abundance (without picophytoplankton), picophytoplankton abundance, Margalef's richness and Pielou's evenness.

PERMANOVA TEST RESULTS				
Main test	Df	SS	Pseudo-F	*p*-value
Habitat	5	2.35×10^5	21.53	0.001
Pairwise tests			Pseudo-*t*	*p*-value
H2-H3			3.85	0.001
H2-H4			5.07	0.001
H2-H5			4.53	0.001
H2-H6			6.92	0.001
H2-H1			3.71	0.001
H3-H4			2.86	0.001
H3-H5			2.76	0.002
H3-H6			3.78	0.001
H3-H1			5.67	0.001
H4-H5			2.38	0.001
H4-H6			5.37	0.001
H4-H1			6.99	0.001
H5-H6			3.48	0.001
H5-H1			5.60	0.001
H6-H1			7.51	0.001

KRUSKAL-WALLIS H TEST RESULTS			
Variable	**Chi-squared**	**Df**	***p*-value**
Total phytoplankton community abundance (without picophytoplankton)	94.68	5	< 0.001
Picophytoplankton abundance	138.41	5	< 0.001
Margalef's richness	133.21	5	< 0.001

Pielou's evenness	64.48	5	< 0.001
Harmful algae abundance	37.47	5	< 0.001

Clear patterns in phytoplankton community abundance and diversity were observed by habitat (Figure 7). Median total phytoplankton abundance (without picophytoplankton) was greater in H1 than all other habitats and lower in H3 and H6 than all other habitats, which did not significantly differ from each other (Figure 7). Large variation in total community abundance was observed in habitats H1–H5, though was most pronounced in H3–H5 (Figure 7A). Median picophytoplankton abundance was significantly greater in H4 and H5 than all other habitats and significantly lower in H1 and H6 than all other habitats (Figure 7B). Median Margalef's richness tended to decrease with increasing salinity, with significantly greater richness in H1 and H2 than all other habitats, and significantly greater richness in H1 than H2 (Figure 7C). Conversely, richness was significantly lower in hypersaline habitats H5 and H6 than all others, which did not significantly differ from each other. Median Pielou's evenness was significantly greater in H6 than in all other habitats, except for H3, where evenness was significantly greater than in H1, H2 and H4 (Figure 7D).

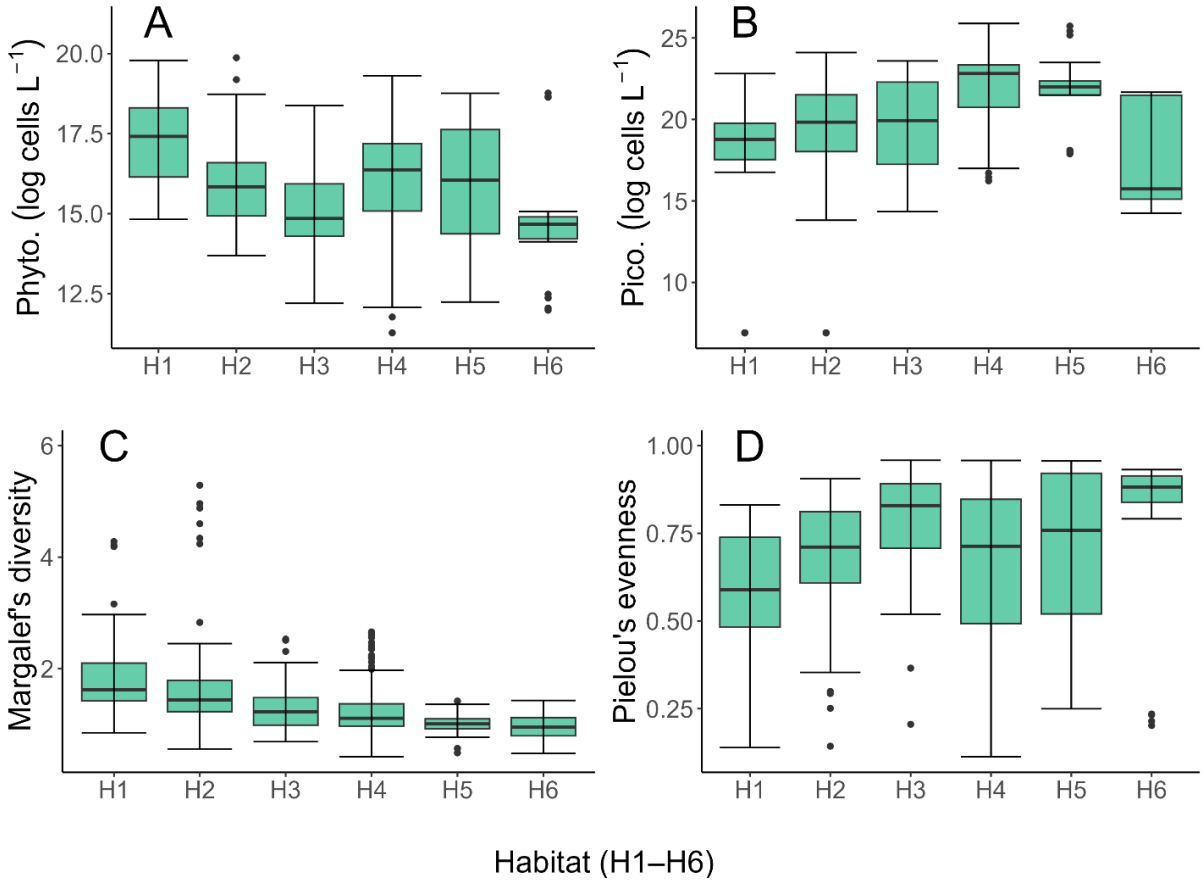

Figure 7. Box- and whisker-plots of (A) total phytoplankton community abundance (without picophytoplankton, (B) picophytoplankton abundance, (C) Margalef's richness and (D) Pielou's evenness by habitat.

The relative abundances of taxonomic groups and species within taxonomic groups largely varied between habitats (Figure 8). Picophytoplankton relative abundance was highest (≥ 95% of total abundance) in brackish–marine H3 and hypersaline H4 and H5 habitats, contrasting with the least and most saline habitats (H1 and H6) where picophytoplankton relative abundance was considerably lower (68% and 75% respectively; Figure 8A). The relative abundance of taxonomic groups without picophytoplankton also demonstrated clear patterns (Figure 8B). Diatoms were consistently more abundant than all other groups across all habitats, apart from H1. Diatoms had the largest relative abundances in H6 (47%), H4 (39%), H3 (38%) and H5 (34%). Dinoflagellates also had higher relative abundances under higher salinity habitats, with their highest relative abundance in extreme hypersaline H6 (43%), followed by H3 (30%), H4 and H5 (both 21%), and the lowest relative abundance in low salinity H1 (3%). In contrast, Cyanoprokaryotes dominated lower salinity conditions, with the highest relative abundance in H1 (37%), but were scarce in higher salinity habitats H3–H6 (≤ 5%). Chlorophytes showed preferences for both low salinity H1 and high hypersaline H5 with their highest relative abundances of 28% in each, while Prasinophytes had their highest relative abundance in H5 (10%) with < 5% relative abundance elsewhere. Cryptophytes had greater relative abundances in freshwater–brackish and marine conditions (H2 = 20%; H3 = 13%; H1 = 10%) than elsewhere (≤ 7%), with decreasing relative abundance with increasing salinity. Chrysophytes, Euglenophytes, Prymnesiophytes and other phytoplankton species had low relative abundances (< 5%) across all habitats.

The relative abundance of phytoplankton species within taxonomic groups also varied across habitats, highlighting dramatic shifts in phytoplankton communities across the salinity gradient (Figure 8C–L). Chlorophytes, Chrysophytes, Cryptophytes, Euglenophytes, Prymnesiophytes and other phytoplankton trended towards increasing simplicity (i.e., fewer species with greater relative abundances) in community composition with increasing salinity. In contrast, Dinoflagellates displayed the opposite trend with only a few species present in lower salinity habitats that were dominated by Gymnodinioids < 20 µm (Figure 8H). Gymnodinioids < 20 µm were the most abundant species group of Dinoflagellates in all habitats except for H6 where *Gyrodinium* spp. and *Protoperidinium* spp. were the two most abundant species respectively. *Gyrodinium* spp. were also well represented across habitats, being the second most abundant Dinoflagellate in H3 and H5 and third most abundant in H1 and H2.

Chlorophytes shifted from a community with more equal relative abundances in H1 and H2 where *Chlorohormidium* sp. was most abundant, to *Chlamydomonas* sp. dominance in H3 and *Koliella* sp. dominance in all hypersaline habitats H4–6 (Figure 8C). *Koliella* sp. increased in relative abundance with increasing salinity, such that it represented 75% and 99% of Chlorophyte abundance in H5 and H6 respectively. Chrysophytes, Euglenophytes and Prymnesiophytes were dominated by *Ochromonas* spp., *Eutreptiella* spp. and *Chrysochromulina* spp. respectively (Figure 8D, I and L). These species were the only representative of these groups in H6, with *Eutreptiella* spp. also the only Euglenophyte in H5. Of the other phytoplankton species group,

Mesodinium rubrum was the most abundant species from H1–4 and second most abundant in H5 but was not present in H6 (Figure 8J). Heterotrophic flagellates were most abundant in H5 and only plankton species in the other group present in H6. *Apedinella spinifera* was the third most abundant species in the other phytoplankton group from H1–4, but was not present in H5 or H6, while *Pedinellid* spp. were the third most abundant in H5 but were not present in any other habitat.

Cryptophytes were mostly represented by *Plagioselmis prolonga*, *Hemiselmis* sp. and *Leucocryptos* sp. (Figure 8E). *Plagioselmis prolonga* was the most abundant Cryptophyte in H1, H4 and H5 but was not present in H6. *Hemiselmis* sp. was the most abundant Cryptophyte in H2, H3 and H6 and was present in all habitats along with *Leucocryptos* sp., which was the second or third most abundant Cryptophyte in all habitats apart from H1.

Prasinophytes showed a distinct shift with increasing salinity, with *Pyramimonas* spp. dominating H1–4 but being the third most abundant in H5 behind *Scourfieldia* sp. and *Mantoniella squamata* and not being present in H6 (Figure 8K). *Mantoniella squamata* and *Scourfieldia* sp. were the most abundant Prasinophytes in H6 with *Tetraselmis* sp. the only other Prasinophyte present. *Tetraselmis* sp. was present in all habitats, being the second most abundant Prasinophyte in H1–4.

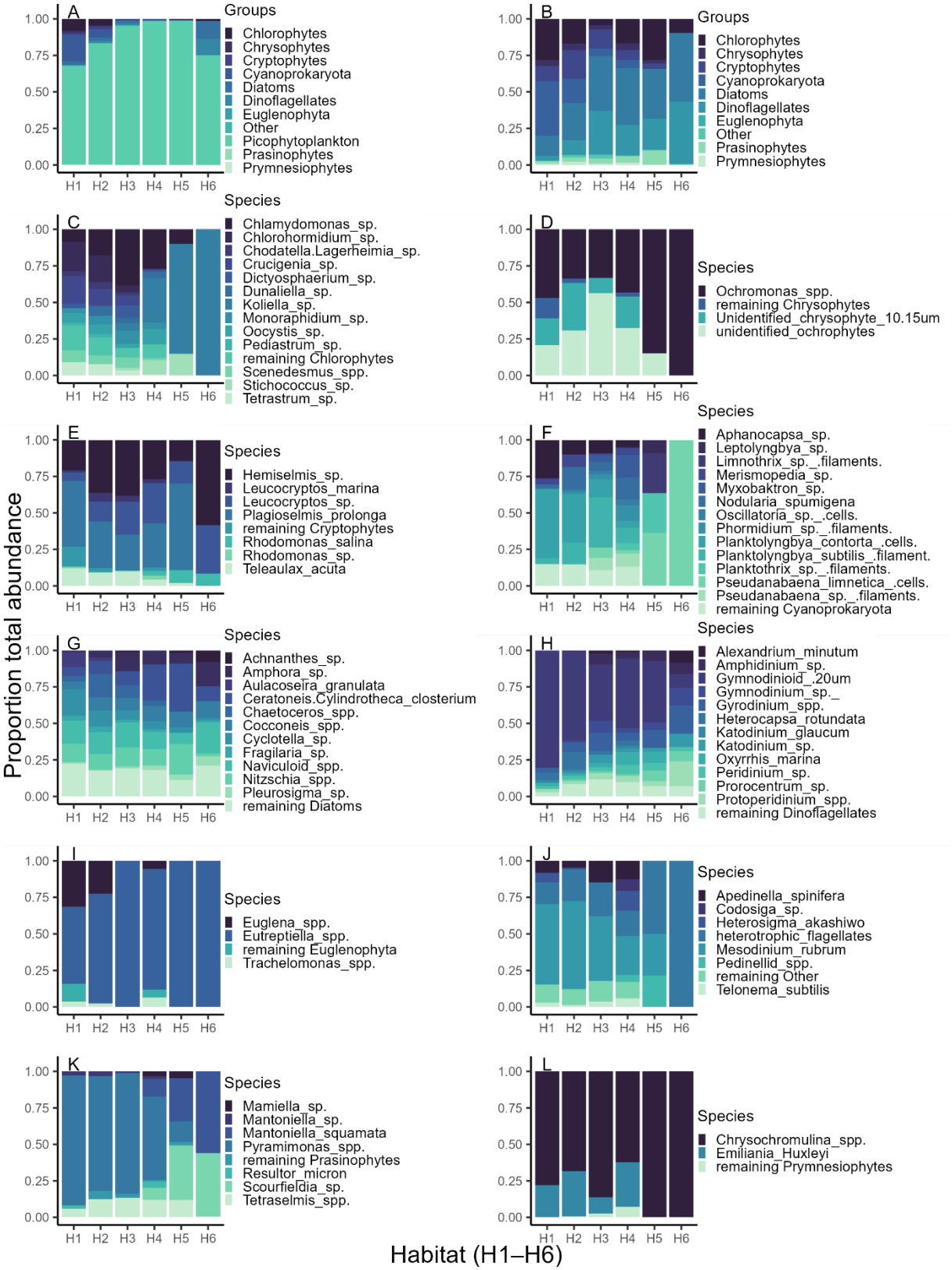

Figure 8. Relative abundance of taxa by habitat. The relative abundance of taxonomic groups within the total phytoplankton community are displayed with (A) and without picophytoplankton (B). The relative abundance of the most abundant species (≥1% of total abundance) within each taxonomic groups are displayed for Chlorophytes (C), Chrysophytes (D), Cryptophytes (E), Cyanoprokaryotes (F), Diatoms (G), Dinoflagellates (H), Euglenophytes (I), Other phytoplankton (J), Prasinophytes (K) and Prymnesiophytes (L).

Cyanoprokaryotes showed complex shifts between habitats with the most even relative abundance in H4 and the least evenness in lower salinity H1 and H2 habitats and hypersaline H5 and H6 (Figure 8F), though Cyanoprokaryote diversity was much greater in H1 and H2 than in H5 and H6. H1 and H2 were dominated by *Planktolyngbya contorta,* with *Planktolyngbya subtilis* the most abundant Cyanoprokaryote in H3. H5 consisted primarily of *Pseudanabaena limnetica*, *Planktothrix* sp. and *Limnothrix* sp. with *Pseudanabaena limnetica* the only Cyanoprokaryote in H6.

Diatoms had the most even relative abundances across all habitats with the most abundant species (> 1% total phytoplankton community abundance) present from H1–6 (Figure 8G). However, the relative abundances of these species did shift between habitats. *Cyclotella* sp was the most abundant in H1, with *Chaetoceros* spp. the most abundant in H2, *Naviculoid* spp. in H3 and H6 and *Ceratoneis/Cylindrotheca closterium* in H4 and H5. *Naviculoid* spp. were well represented in all habitats, being the second most abundant Diatom in H1, H2 and H4. *Nitzschia* spp. were also well represented in all habitats except H6, being the second most abundant Diatom in H3 and the third most abundant Diatom in H1, H2, H4 and H5. *Amphora* sp. and *Cocconeis* spp. relative abundances increased with salinity, being the second and third most abundant species in H6 respectively.

3.4 Predicting harmful algae

Harmful algae abundance significantly differed by habitat (Table 8), with a greater mean HAB abundance in H1 than all other habitats and a lower abundance in H6 than all other habitats (Figure 9). The mean HAB abundance in all habitats was far lower than all risk levels (e.g., H1 = $2.6 \times 10^5 \pm 6.0 \times 10^4$; Low risk level = 5×10^6 cells L^{-1}; Figure 9A). However, the mean abundances of *Alexandrium* spp. (Figure 9B) and *Gymnodinium* sp. (Figure 9C) were greater than the action level (Table 2) in H6 and greater than the alert level in H3, H4 and H5 for both species, with the mean abundance of *Gymnodinium* also surpassing the alert level in H2.

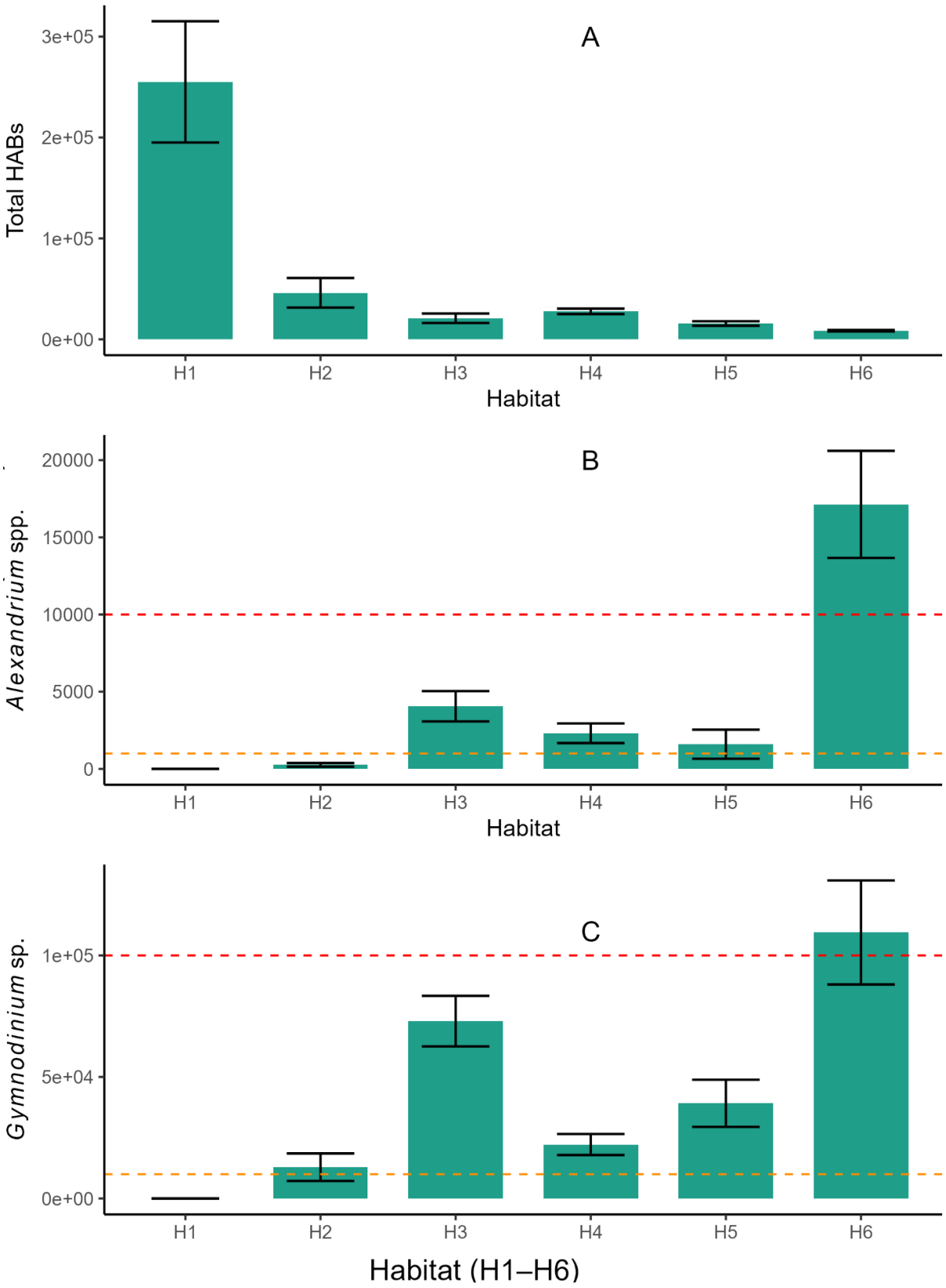

FIGURE 9. MEAN ABUNDANCES (CELLS L^{-1}) OF (A) TOTAL HARMFUL ALGAE COMMUNITY, (B) *ALEXANDRIUM* SPP. AND (C) *GYMNODINIUM* SP. BY HABITAT WITH STANDARD ERROR BARS IN BLACK. HORIZONTAL LINES INDICATE SPECIES SPECIFIC ALERT (YELLOW) AND ACTION (RED) LEVELS.

The XGBoost model performed well, explaining 77% of the variation in harmful algae abundance (R^2 = 0.77), with a MAE of 3.05 x 10^6 and an RMSE of 1.09 x 10^7 that represents 5.66% error relative to the range of observations. The observed vs predicted model values were strongly and significantly correlated (R^2 = 0.89; t = 19.30, df = 102, p < 0.001), though with some deviation from the 1:1 line, particularly at very high abundances (Figure 10A). The majority of the observations are located within relatively lower abundances (maximum 1.7 x 10^7 cells L^{-1} ; Figure 10B), where most predictions fall close to the 1:1, though some scatter is still visible.

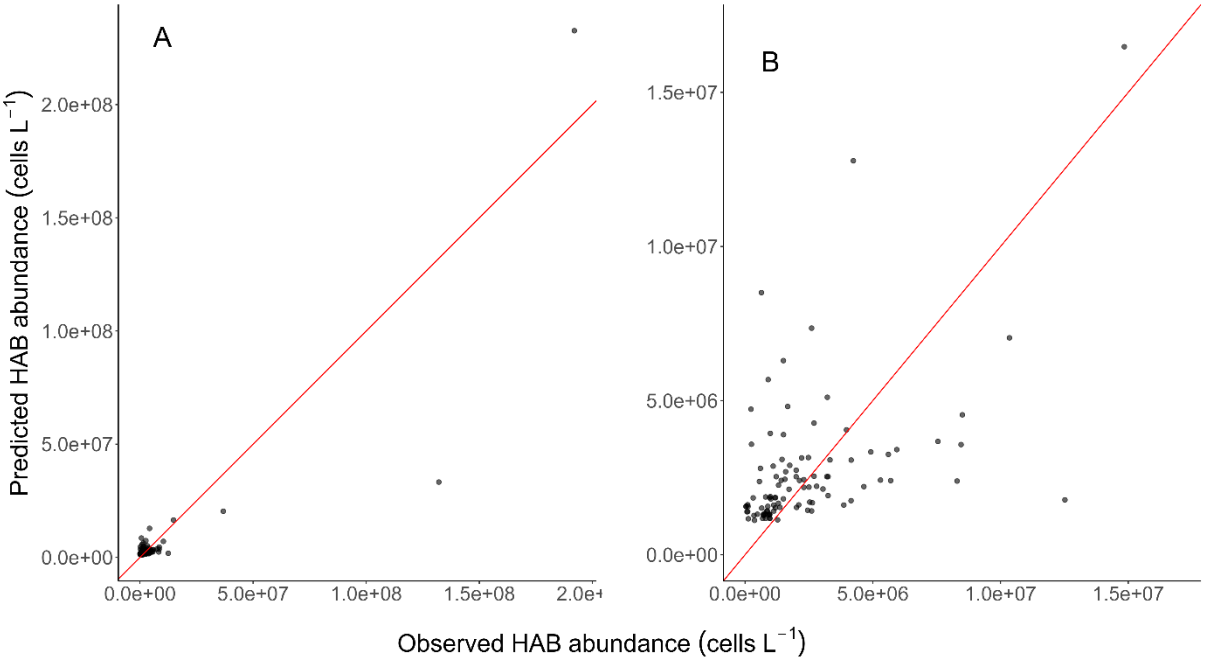

Figure 10. XGBoost model predictions plotted against observed HAB abundance showing the whole range of values (A) and within a range where the majority of the values lie (< 1.7 x 10^7 cells L^{-1}; B).

Mean SHAP values highlighted that salinity was the most important variable in the XGBoost model predicting HAB abundance (Mean SHAP = 0.48), with pH the second most important variable in the model (mean SHAP = 0.25), followed by NO_X and distance from Murray Mouth (mean SHAP = 0.16 for both; Figure 11A). Salinity had an overall negative impact on HAB abundance, as indicated by the large amount of negative SHAP values, with positive SHAP values only when salinity was low (Figure 11B). pH also had a largely negative impact on HAB abundance. NO_X had an increasingly positive impact on HAB abundance with higher values, while distance from Murray Mouth was the opposite.

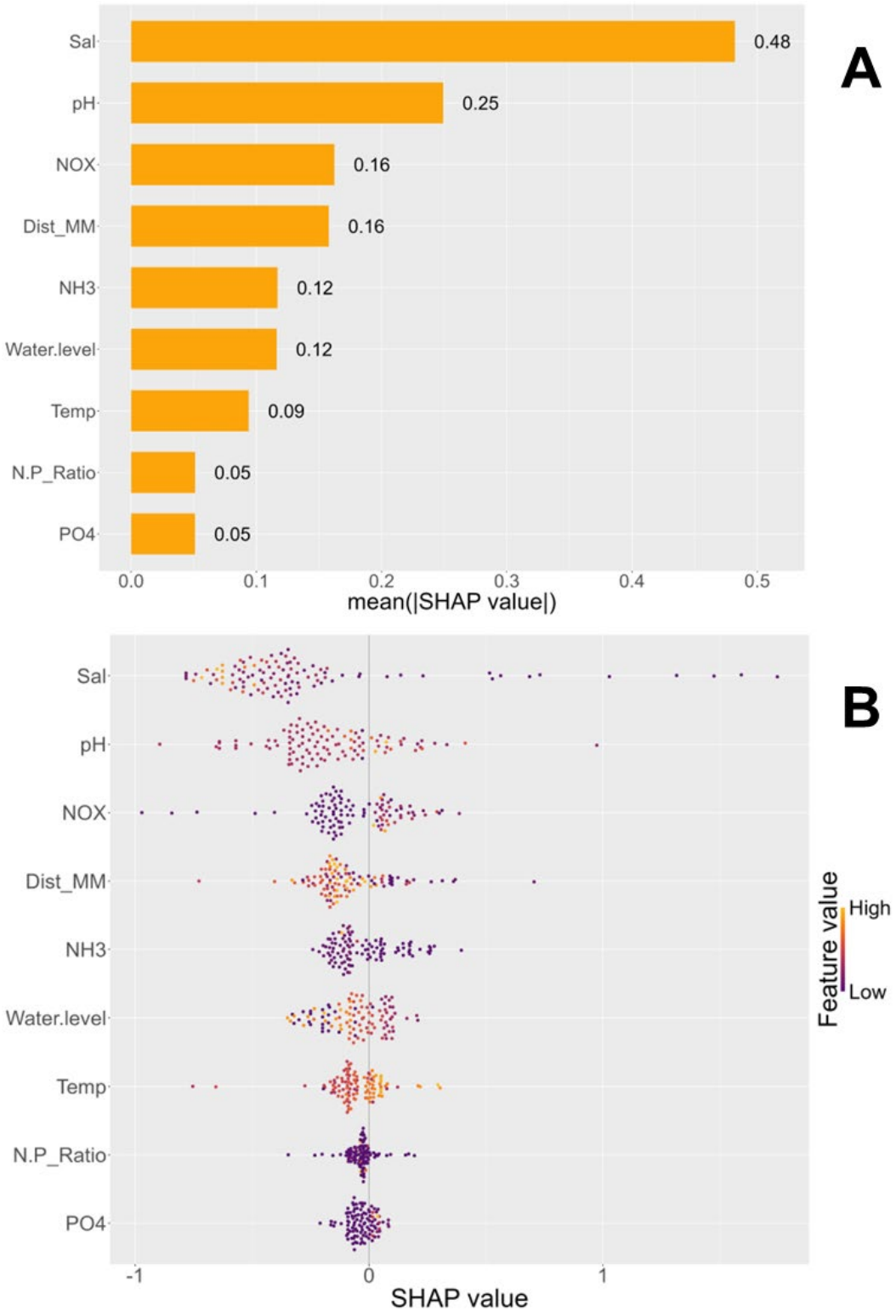

Figure 11. Mean SHapley Additive exPlanation (SHAP) scores (A) and bee swarm plot showing the distribution of SHAP values(B) for each environmental predictor variable used in the XGBoost model predicting total HAB abundance. Environmental variables are ordered from most to least important (highest to lowest mean SHAP value). The bee swarm plot indicates how each SHAP value of the predictor variable has an increasing (positive), neutral (near zero) or decreasing (negative)effect on HAB abundance. The colouring of these points indicate the value of the predictor variable, from low (dark purple) to high (bright yellow).

4 Discussion

4.1 Flow periods shape the Coorong ecosystem

Climate-driven flow conditions strongly shaped the Coorong's environmental conditions and phytoplankton communities. The flow periods captured in this study covered a large gradient of conditions, from extreme dry, whereby the Coorong experienced the worst drought on record for South-eastern Australia (the Millennium Drought) and received little to no freshwater inputs (Brookes et al., 2023), to extreme wet (Keneally et al., 2025). The importance of freshwater flows for the ecological functioning of the Coorong has been well documented, including for environmental conditions such as salinity (Brookes et al., 2023; Brookes et al., 2022; Webster, 2010b), sediment character and greenhouse gas production (Keneally et al., 2024; Lam-Gordillo, Huang, et al., 2022), water quality and eutrophication (Huang et al., 2024; Mosley et al., 2023; Priestley et al., 2022). These flows are also supporting a wide range of organisms including macrophytes (Kim et al., 2015; Paton et al., 2015), fish (Brookes et al., 2015; Brookes et al., 2022), waterbirds (Paton et al., 2009a; 2009b), micro- and macro-invertebrates (Dittmann et al., 2015; Hemraj et al., 2017; Lam-Gordillo, Mosley, et al., 2022) and the phytoplankton community (Hemraj et al., 2017; Jendyk et al., 2014; Leterme et al., 2015). Here, we furthered our understanding of the importance of climate conditions mediating freshwater inputs for the Coorong ecosystem and how it drives changes in the phytoplankton community. The analyses covered a much greater timespan and captured a greater range of climatic conditions than previous studies investigating responses of the phytoplankton community (e.g., Jendyk et al., 2014; Leterme et al., 2015; Schapira et al., 2010), demonstrating the comprehensiveness of our results in revealing phytoplankton community responses across the full extent of possible climate conditions.

4.2 Environmental drivers of phytoplankton community abundance and diversity

Through multiple methods of analyses, both salinity and water level were revealed as the principal drivers of changes in phytoplankton community abundance, diversity and assemblage. This aligns with existing literature highlighting salinity and water level as master environmental variables for shallow lake and lagoon ecosystem functioning globally (Keneally et al., 2024; McGrath et al., 2025), with both variables demonstrated as being highly important for structuring phytoplankton communities in shallow lakes and lagoons worldwide (Larson and Belovsky, 2013; Leira and Cantonati, 2008; Sun et al., 2022; Tunca et al., 2024) and in the Coorong (Jendyk et al., 2014; Leterme et al., 2015; Leterme et al., 2013; Schapira et al., 2010).

Distance from Murray Mouth and temperature were also consistently impacting on the structure of phytoplankton communities, but to a lesser degree. The remaining environmental variables (NH_3, NO_X, N:P, pH and PO_4) were significant in distance-based linear modelling and some generalised additive models but with a weak effect. Salinity and water level were inversely correlated to each other, with both variables

strongly determined by the volume of freshwater inputs, whereby water level increases and salinity decreases in response to greater freshwater inputs (Brookes et al., 2022; Webster, 2010b). Water temperature was also inversely correlated to water level, demonstrating the increased heating effect from concentrated solar radiation in a smaller volume of water under lower water levels (Zhang et al., 2024), particularly evident during the hotter and drier conditions of the drought.

Distance from Murray Mouth was positively correlated with salinity, highlighting the salinity gradient that characterises the Coorong ecosystem (Brookes et al., 2022; Mosley et al., 2023; Webster, 2010b). However, the spatial character of the Coorong also consists of variable hydrodynamic conditions which can affect phytoplankton community structure (Deng et al., 2024). Locations closer to the Murray Mouth experience a combination of freshwater flow and tidal velocity signals coupled to periodic wind forcing over a range of varying temporal scales (e.g., daily, seasonal, interannual) (Huang et al., 2024; Webster, 2010a, 2010b) dictating complex water circulation processes and shorter residence times that can affect phytoplankton dynamics (Chen et al., 2023; Deng et al., 2024). While in locations further away from the Murray Mouth, particularly in the South Lagoon, hydrodynamics and water circulation processes are primarily wind-driven due to the narrow channel constriction separating North and South Lagoons at Parnka Point (Figure 12), with residence times much longer (Huang et al., 2024; Webster, 2010b).

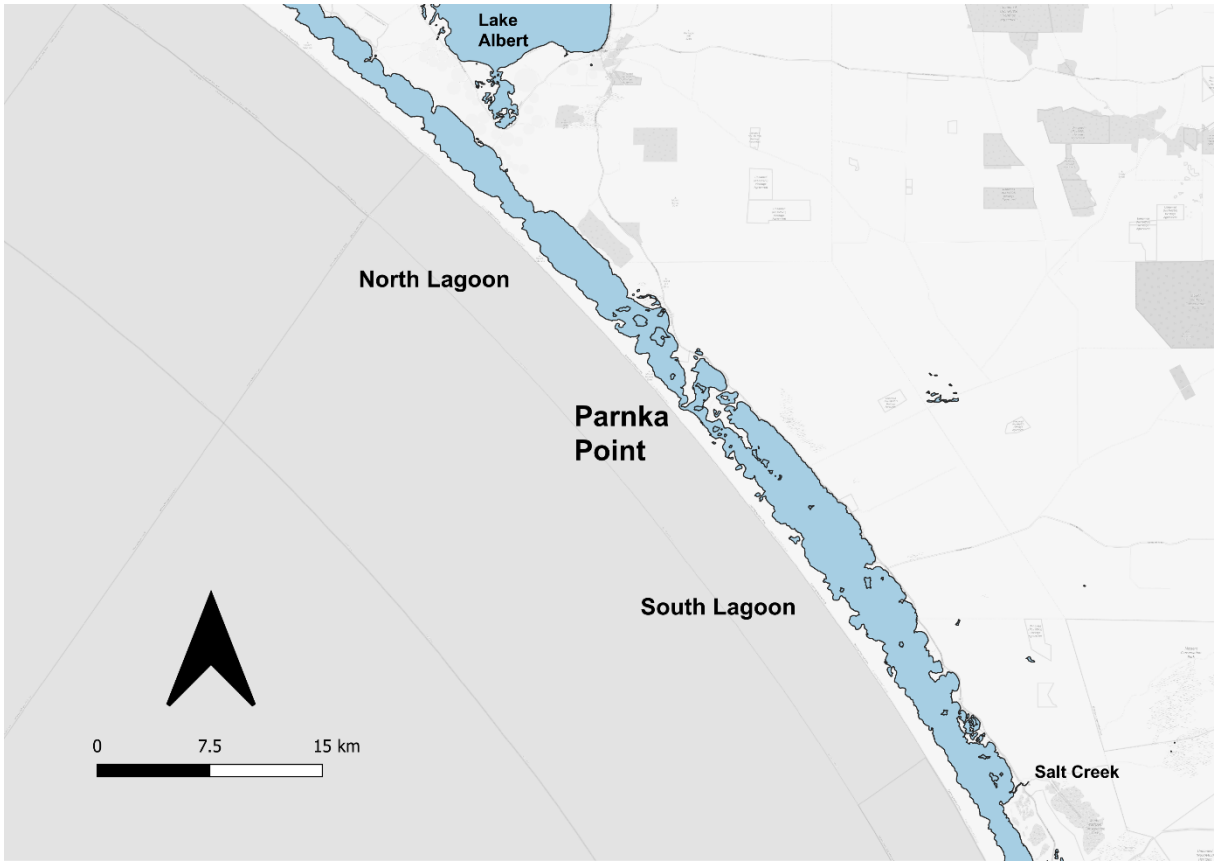

Figure 12. Map of the Coorong highlighting the relatively narrow ~100 m wide constriction at Parnka Point that separates the North and South lagoons.

4.3 The effects of salinity on the phytoplankton community

Salinity typically has a negative impact on phytoplankton species richness (Larson and Belovsky, 2013; Sun et al., 2022; Tunca et al., 2024) and total community abundance (Tunca et al., 2024), aligning with our observations. Tunca et al. (2024) observed a decline in richness and abundance from freshwater to marine conditions, following a similar trajectory to that observed in Figure 7. High salinity creates osmotic stress that is lethal for many lower salinity-adapted species, limiting the number of species that can survive (Flöder et al., 2010). The resulting community is characterised by low species richness, but can have relatively high evenness because the dominant species are able to persist, leading to a community where few species contribute relatively equally to the total abundance (Flöder et al., 2010; Sun et al., 2022) or low evenness with a community dominated by a few salt-tolerant species (Larson and Belovsky, 2013). Here, we observed an overall positive trend between evenness and salinity, with the greatest evenness under extreme hypersaline conditions (≥ 120 PSU) with elevated evenness in marine and high hypersaline conditions (85–119 PSU) and the lowest evenness under low salinities (< 5 PSU). Elevated evenness in marine conditions can represent a relatively stable ecosystem (Remmert, 1969), allowing for long evolutionary histories of the organisms which fill the niches within these habitats (Telesh et al., 2013). Higher phytoplankton community abundance and richness but lower evenness in low salinities (< 5 PSU) may be a result of the interaction between salinity and nutrients, with higher inflows reducing salinity and importing nutrients to the system (Lakane et al., 2025; McGrath et al., 2025; Winder and Sommer, 2012). The increased nutrient supply coupled to reduced salinity increases overall diversity (Larson and Belovsky, 2013), but decreasing salinity also lowers evenness allowing for increased dominance of individual species. Furthermore, the lower salinity habitats in the Coorong are highly dynamic environments driven by the mixing of seawater and freshwater (Webster, 2010a, 2010b). These conditions limit individual species dominance as communities need to have a growth rate that exceeds water residence time if they are to persist and develop stable communities adapted to the local conditions (Jendyk et al., 2014; Leterme et al., 2015).

Contrary to the total community abundance without picophytoplankton, picophytoplankton abundance increased with increasing salinity up to extreme hypersaline conditions (~ 120 PSU), then dropped sharply. A similar pattern was also observed in the Coorong by Schapira et al. (2010) where picophytoplankton abundance increased with increasing salinity up to ~ 110 PSU, then declined when salinity > 120 PSU. Picophytoplankton abundance has also been shown to increase with increasing salinity in saline lakes in Romania (Somogyi et al., 2014) and Tunisia (Elloumi et al., 2009). Picophytoplankton have a selective advantage over larger phytoplankton species in aquatic habitats with high salinity and turbidity due to reduced grazing pressure as there are fewer predators (Pedros-Alio et al., 2000; Somogyi et al., 2022). In addition, the strong light limitation in highly turbid water gives picophytoplankton a competitive advantage over larger algae due to their superior light-harvesting efficiency in low-light conditions (Alegria Zufia et al., 2021; Callieri et al., 2007; Malinsky-Rushansky et al., 2002). However, a limit to their competitive

advantage and salinity tolerance was observed in our study and by Schapira et al. (2010) when salinity reached 120 PSU. Although not identified to species level in this study, the picophytoplankton community in the Coorong predominantly consist of the Cyanobacteria genus *Synechococcus* (Jamieson et al. 2022; Priestly et al. 2022).

4.4 The effects of water level on the phytoplankton community

Water level fluctuations have been observed to have mixed effects on phytoplankton communities in shallow lakes and lagoons (Cardoso et al., 2012; da Costa et al., 2015; Leira and Cantonati, 2008). Drawdown can both stimulate or decrease phytoplankton abundance, depending on the depth of the lake, the amount of sediment resuspension that occurs and the subsequent increase or decline in macrophyte biomass (Bakker and Hilt, 2015; da Costa et al., 2015). For example, in the semi-arid shallow Lakes Pocinhos and ESEC, Brazil, mixed responses were observed whereby phytoplankton abundance increased due to increasing evapoconcentration of nutrients in the deeper Lake Pocinhos, but in the shallower Lake ESEC, phytoplankton abundance declined on drawdown as turbidity increased due to increased resuspension (da Costa et al., 2015). Similarly, phytoplankton diversity also shows mixed responses to water level decline, with diversity and richness both observed to increase (Cardoso et al., 2012; da Costa et al., 2015) or decrease in response (da Costa et al., 2015; Lakane et al., 2025). Increases in water level can decrease phytoplankton abundance due to the dilution effect (Cardoso et al., 2012; Pan et al., 2018; Wang et al., 2022), though may also result in increases in abundance due to increased nutrient availability from the inflowing water (Leira and Cantonati, 2008; Loverde-Oliveira et al., 2009). Additionally, higher water levels can also increase phytoplankton diversity, including Margalef's richness (Deng et al., 2024) and Pielou's evenness (Wang et al., 2022). In our study, water level increased total community abundance and richness, but decreased evenness, having the inverse effect of salinity. This was likely due to the combined effects of decreasing salinity coupled with increasing nutrient supply due to greater freshwater inputs from the River Murray (Mosley et al., 2023). Additionally, this may be the result of hydrological transport of lower salinity-adapted species from upstream in the River Murray to the Coorong, which persist in freshwater–low brackish H1 that represent ~ 20% of the Coorong under extreme wet and wet conditions.

4.5 Salinity-derived habitats provide a strong basis for characterisation of phytoplankton communities

Non-linear responses of phytoplankton community abundance, diversity and community composition were observed along the temporally fluctuating salinity gradient that defines the Coorong ecosystem (Figure 7). This aligns with previous studies of phytoplankton communities in the Coorong (Jendyk et al., 2014; Leterme et al., 2015) and suggests varying species tolerances and threshold values where shifts in species composition occur (Flöder et al., 2010; Winder and Sommer, 2012). As such, our results justify the delineation of phytoplankton communities into salinity-derived habitats, as demonstrated by distinct patterns in phytoplankton communities observed under different habitats.

Similar to the results of Leterme et al. (2015) and Jendyk et al. (2014), we observed a dominance of Diatoms and Dinoflagellates under extreme hypersaline conditions (H6), with Diatoms also being the most abundant group in H3 and H4. We also observed a greater abundance of Chlorophytes in lower salinity habitats H1 and H2, as observed by Leterme et al. (2015) and Jendyk et al. (2014). However, contrary to Leterme et al. (2015) and Jendyk et al. (2014), H1 was dominated by Cyanoprokaryotes, not Chlorophytes, with Chlorophytes the second most abundant group. This difference is largely the result of increased Cyanoprokaryote abundance and diversity during the extreme wet period, with this period having abundant low salinity habitat and was not captured by Leterme et al. (2015) and Jendyk et al. (2014). Chlorophyte abundance was also high in hypersaline H4 and H5, where Chlorophytes were the third and second most abundant group respectively (Figure 8). This differs to Leterme et al. (2015) and Jendyk et al. (2014) because the dry period was not captured by these studies, a period where Chlorophytes, primarily *Koliella* sp. and *Chlamydomonas* sp., were highly abundant. The above differences demonstrate the importance of capturing phytoplankton community dynamics over a large temporal scale that captures a full extent of climate conditions. This increases our understanding of phytoplankton community responses to varying environmental conditions and improves predictions of phytoplankton community dynamics under future climate conditions, when coupled to hydrodynamic model outputs that forecast key environmental variables such as salinity.

4.6 Hydrological change

Salinity and water level are directly influenced by the quantity of freshwater inputs to the Coorong and by Southern Ocean tidal inputs, which is in turn, dictated by the degree of mouth opening (Webster, 2010b). Historically, the degree of connection to the ocean was determined solely by the quantity of freshwater inputs, but now remains open due to dredging to maintain hydrological flushing of the Coorong and connectivity for passage of motile organisms, such as diadromous fish and seals (Brookes et al., 2015; Brookes et al., 2023). Under historical conditions, the Murray Mouth was closed 1% of the time, but currently without dredging, would be closed up to 40% of the time due to reduced freshwater inputs (Kingsford et al., 2011). Freshwater flow travelling down the River Murray has declined due to large-scale development of irrigated agriculture within the Murray-Darling Basin (Brookes et al., 2023; Kingsford et al., 2011; Mosley et al., 2023) and due to climate change-induced decreases in rainfall across South-eastern Australia (Timbal et al., 2017).

With increasing climate change and continued agricultural productivity in the Murray-Darling Basin, freshwater inputs are predicted to continue to decrease over time up to a point of hydrological minimum with concomitant increases in salinity and decreases in water level and hydrological flushing (Rees et al., 2022; Timbal et al., 2015). Under these dry and extreme dry climate conditions, much of the Coorong will be experiencing hypersalinity, with the lowest salinities in high brackish to marine. Our predictions suggest that under these elevated salinity conditions, phytoplankton diversity will be low with abundances high, particularly of picophytoplankton, up until

extreme hypersalinity ≥ 120 PSU when phytoplankton abundance will decline due to osmotic stress (Flöder et al., 2010; Leterme et al., 2015). With the majority of the Coorong in salinities > 40 to 120 PSU, the phytoplankton community will be dominated by Diatoms, Dinoflagellates and several Chlorophyte species with very high picophytoplankton abundance.

4.7 Phytoplankton response

With increasing salinisation of the Coorong, H1 and H2 habitats and associated phytoplankton communities will diminish, except sporadically under future higher flow events. During these events, phytoplankton communities in the lowest salinity H1 are predicted to be dominated by Cyanoprokaryotes (predominantly *Planktolyngbya contorta* and *Aphanocapsa* sp.) and Chlorophytes (*Crucigenia* sp, *Scenedesmus* spp., *Oocystis* sp. and *Tetrastrum* sp.). H1 communities may be transient as conditions return to a pre-flood state with increasing salinity promoting picophytoplankton, Diatom and Dinoflagellate abundances, and Chlorophyte diversity decreasing with a shift to *Koliella* sp. and *Chlamydomonas* sp. dominance. The phytoplankton community within brackish H2 is predicted to have the most even representation of taxonomic groups of all the habitats, with similar relative abundances of Diatoms, Cryptophytes, Chlorophytes and Cyanoprokaryotes, high species richness and moderate evenness. Typically, brackish H2 represents unstable estuarine conditions with fluctuating salinity and tends to have low overall species diversity, though can have high abundances of a few species that are well adapted to the fluctuating conditions (Karpowicz et al., 2023; Mironova et al., 2013). However, our observations contradicted this tendency displaying relatively higher species richness and more equal representation of taxonomic groups in H2 (Figure 8). This may be the result of salinity fluctuations promoting diversity by creating transient niches that different species can exploit, preventing competitive exclusion over time (Flöder and Burns, 2004). Coupled to this, increased nutrient supply with higher river inflow can alleviate salinity limitations and support greater diversity (Li et al., 2021). The Coorong will consist of approximately one-fifth H2 under intermediate, wet and extreme wet climate conditions. Like H1, and its associated phytoplankton community will be largely lost from the Coorong under dry and extreme dry climate conditions, highlighting the importance of freshwater inputs for maintaining phytoplankton species diversity.

4.8 Food web consequences

A reduction in the overall diversity of phytoplankton will impact the Coorong food web as species important for the diets of higher trophic organisms disappear (Henson et al., 2021). Trophic energy transfer efficiency will decrease as interactions shift from phytoplankton–zooplankton dominated to bacteria, viruses and picoplankton dominated interactions with a shift towards heterotrophy (Hemraj et al., 2017). In addition, the higher total phytoplankton abundance, predominantly picophytoplankton, will further impact the food web as benthic light availability will decrease, limiting light for the submerged macrophyte community causing significant decreases in macrophyte distribution and abundance (Le Fur et al., 2019; Yang et al.,

2023). The *Ruppia tuberosa* submerged macrophyte community is considered a key ecosystem element in the Coorong due to its importance for water quality maintenance, sediment trapping and stabilisation, and for primary production, providing an essential carbon source to the Coorong food web (Nicol, 2005; Paton et al., 2015). It provides essential habitat and foraging substrates for waterbirds, fishes and invertebrates (Asanopoulos and Waycott, 2020; Paton et al., 2015), provides a source of detritutus for detritivores (Nicol, 2005) and is an important component in the diet of waterfowl and fish species (Giatas et al., 2018; Paton et al., 2015). Future decreases in freshwater inputs and water levels coupled to increases in salinity will further impact the submerged macrophyte community through increases in osmotic stress and increased exposure to desiccation (Kim et al., 2015). The impacts of a future dominated by a hydrological minimum will be far reaching within the Coorong, not only for primary producers, but for the entire system as salinisation and eutrophication intensify resulting in a severely degraded ecosystem state (Mosley et al., 2023), as observed during the final years of the Millennium Drought (2007–2010) when no flows entered the Coorong (Kingsford et al., 2011).

Sea-level rise may compensate for declines in connectivity and water level with salinity becoming more marine, as the Coorong ecosystem becomes increasingly influenced by tidal inputs (Rees et al., 2022; Timbal et al., 2015). A future state of high ocean exchange may produce a greater proportion of high brackish–marine H3 and reduce the importance of freshwater flows controlling salinity and water level in the Coorong, particularly in the north lagoon. We predict phytoplankton communities in H3 to be dominated by Diatoms and Dinoflagellates, though with an overall moderate species richness and high evenness where Cryptophytes (e.g., *Hemiselmis* sp, *Leucocryptos* sp. and *Plagioselmis prolonga*), Prasinophytes (*Pyramimonas* spp.) and Cyanoprokaryotes (*Aphanocapsa* sp., *Planktolyngbya contorta* and *Myxobaktron* sp.) will still be present in relatively high abundances. However, Chlorophytes are predicted to be largely absent under these conditions and picophytoplankton will be dominant, representing 95% of the total community. In addition, without freshwater inputs to the system, large parts of the Coorong, particularly the hydrologically restricted South Lagoon, are likely to remain in hypersaline conditions (Lester et al., 2013), thus the Coorong will still largely be in an ecologically degraded state with reduced biological diversity and high turbidity (Mosley et al., 2023).

4.9 XGBoost model

The XGBoost model generally performed well explaining 77% of the variation in total HAB species abundance and a low prediction error relative to the range of observed values (5.7%). Aligning with other analyses, salinity was highlighted as the principal driver of HAB community dynamics, demonstrating the importance of salinity on shaping the Coorong's phytoplankton community abundance, diversity and composition. Contrary to most other statistical analyses performed in this study, pH was observed as the second most important variable explaining HABs. pH had an overall negative impact on HAB species abundance, though with no clear pattern how changing pH affects HAB formation. This aligns with the literature, as the effects of pH

on HAB formation remains unclear (Wells et al., 2020). NO_X and distance from Murray Mouth were the next most important variables, with similar mean SHAP values highlighting an equal amount of influence on HAB abundance. Higher NO_X concentrations had a positive effect on HAB abundance, with nutrient supply recognised as a primary driver of increased frequency, intensity and duration of HABs globally (Anderson 2012). The negative impact of increasing distance south from Murray Mouth on HAB abundance is likely to be a function of increasing salinity, though may also be due to a greater distance from potential sources of HAB species intrusions into the Coorong from freshwater and marine environments.

The XGBoost model has been developed as an initial tool towards predicting HABs in the Coorong into the future. Despite generally good performance, improvements in predicting HAB abundance could be made, particularly as the model tended to underpredict when observed abundance was extremely large (> 1.0 x 10^8 cells L^{-1}). Model performance can be improved by further tuning hyperparameters, increasing explanatory predictors and/or training separate models for low and high HAB abundances. With these improvements, the XGBoost model developed here could be applied to more specific applications, such as predicting the abundance of specific species or taxonomic groups, e.g., toxic Cyanobacteria, that pose a higher risk.

4.10 HAB risk

The risk from harmful algal blooms (HABs) observed in this Coorong dataset is generally considered low, given there were only a few occasions where HAB abundances spiked to levels of high abundances, with the most prolonged bloom occurring in 2012 due to several toxic Cyanobacteria. The highest abundances of HAB species are most likely to occur in lower salinity habitats H1 and H2, predominantly due to the high abundances of toxic Cyanobacteria in these habitats, though these abundances are typically significantly less than the lowest risk level outlined by NHMRC (2008) by an order of magnitude or more. However, it is important to highlight that there is a risk from toxic Cyanobacteria blooms in these lower salinity habitats in the North Lagoon. With increasing distance south from the Murray Mouth, the risk significantly reduces as increasing salinity was observed to have a negative impact on Cyanobacteria. Lower salinity habitats are most prominent under higher flow conditions with increased hydrological flushing. Increased flushing reduces water residence time which will assist in flushing out the HAB and the toxins that are produced (Londe et al., 2016). As such, the overall risk from toxic Cyanobacteria blooms is present, but considered low for the Coorong.

The abundances of most HAB species with specific risk levels (Table 2) have not regularly surpassed these levels. However, the elevated abundances of the genera *Alexandrium* and *Gymnodinium* during the extreme dry period is a cause for concern if a drought was to reoccur. This highlights that despite overall low abundance of HABs during the extreme dry period when the greatest proportion of extreme hypersaline H6 occurred, specific harmful algae species can proliferate to levels which could cause harm. *Alexandrium* species are recognised globally as one of the most

important Dinoflagellate HAB genera due to the severity, diversity and distribution of bloom impacts (Anderson et al., 2012). *Alexandrium minutum*, the sole species responsible for the bloom during the drought, is known to produce saxitoxins, though not all strains produce toxins (Balech 1989). Saxitoxins are potent neurotoxins and a human health risk if ingested from infected shellfish. They can cause paralytic shellfish poisoning (PSP) by binding to nerve cell sodium channels and blocking nerve impulse transmission (Deng et al., 2025). Similar to *Alexandrium* spp., *Gymnodinium catenatum* is also known to produce neurotoxins that can cause PSP (Cunha et al., 2024). The *Gymnodinium* sp. observed in this dataset was not identified to a specific species, thus it is unsure whether this was *G. catenatum* and it cannot be assumed that this *Gymnodinium* species poses a risk.

A limitation of this study is the taxonomic resolution of the Gymnodinioids <20 µm group, which likely comprises multiple species with differing ecological strategies. Gymnodinioids can exhibit autotrophic, heterotrophic, or mixotrophic nutritional modes, and while some taxa are potentially harmful, others are not (Jamieson et al., 2022). Consequently, the ecological significance and HAB risk associated with this group cannot be fully resolved from the available data. Future monitoring should seek to identify Gymnodinioids to species level using molecular and/or advanced microscopy techniques to improve understanding of their ecological function and potential management significance within the Coorong ecosystem.

A further limitation of this study is that toxin concentrations were not measured and as a result, our assessment of harmful algae risk is based solely on phytoplankton cell counts rather than toxin thresholds. For example, *Alexandrium* and *Gymnodinium catenatum* have risk alert levels of 0.8 mg kg^{-1} saxitoxin equivalent (Barua et al., 2020), while the risk level for *Karenia cristata* is 0.8 mg kg^{-1} brevetoxin equivalent (Hort et al., 2021). Microcystins are potent hepatoxins produced by certain Cyanobacteria (primarily by *Microcystis aeruginosa*), with risk alert levels of 1 µg L^{-1} oral drinking water consumption, 39 µg kg^{-1} for fish or prawns and 83 µg kg^{-1} for molluscs (WHO 2022). These toxin-based thresholds highlight that actual risk is more directly linked to toxin production and exposure pathways than to cell abundance alone. It is therefore recommended that future monitoring incorporate toxin measurements alongside phytoplankton cell counts to improve the identification and assessment of risks associated with harmful algal species.

Despite the general low risk of HABs occurring in the Coorong, it is important to document the HAB forming species present and the potential risk they pose. This is exceptionally pertinent given the ongoing and unprecedented *Karenia* spp. bloom in the coastal waters of South Australia. *Karenia* spp. were observed in this dataset, but in abundances that are well below risk levels (Table 2). However, given the right conditions, any HAB species may proliferate causing severe ecological, economic and social damage (Anderson 2012; Wells et al., 2020). For example, certain *Karenia* species (e.g., *K. brevis* and *K. cristata*) produce brevetoxins that when inhaled can cause severe respiratory illness and can bioaccumulate in shellfish causing neurotoxic shellfish poisoning to consumers (Hort et al., 2021). As climate change continues to modify aquatic environments in novel and atypical ways (Staudinger et al., 2021),

future phytoplankton responses to these conditions will be harder to predict. Regular and continued monitoring will improve these predictions by supporting model development. The many gaps in this dataset show that in many instances, particularly during the extreme dry period when sampling occurred for only two months, and during the six years when no data was obtained between the intermediate and dry periods, critical information on phytoplankton dynamics were not captured. This highlights the need for regular monthly monitoring of phytoplankton across the length of the salinity gradient to support predictive tools, early detection and management of HABs into the future.

4.11 Future work

The characterisation of phytoplankton communities by salinity-derived habitats in this study could be supported by an analytical approach following Dang et al. (2025) and use threshold indicator taxa analysis (TITAN) combined with K-prototype clustering to characterise phytoplankton communities under varying environmental gradients. This approach may yield finer ecological resolution of community structure. TITAN combines change-point analysis with indicator species analysis to summarise species occurrence across multiple environmental gradients (Baker and King, 2010). Results of TITAN can be subsequently combined with trait information and fed into K-prototype clustering analysis to identify distinct phytoplankton groups based on ecological characteristics of the phytoplankton community, taking into account the local conditions (Dang et al., 2025). Outputs of these analyses may be applied to process-based aquatic ecosystem models to improve model performance in forecasting phytoplankton communities under future climate scenarios.

Only environmental drivers of phytoplankton community were investigated in our study, but biological drivers of phytoplankton community dynamics, such as species interactions, could be investigated in future work. Species interactions can act as top-down controls via grazing, mortality by viral lysis, competition for resources, such as light and nutrients, and through mutualistically beneficial relationships (Liu et al., 2022). These interactions may be revealed by co-occurrence network-based analyses (e.g., Boyse et al., 2025; Hemraj et al., 2017) to highlight both positive and negative relationships between taxa.

Full molecular characterisation of dominant HAB taxa should be incorporated into future monitoring programs. Molecular approaches would improve taxonomic resolution of morphologically similar groups, including small dinoflagellates and other potentially harmful taxa that cannot be reliably identified to species level using routine light microscopy (Jamieson et al., 2022). This would enable more accurate assessment of species composition, ecophysiological traits and harmful bloom potential, while improving understanding of toxin-producing species and their associated risks within the Coorong ecosystem. Molecular characterisation would also support the development of more targeted monitoring and management strategies for harmful algal blooms.

5 Conclusion

By examining 16 years of data (2007–2023) spanning drought to flood conditions, our study illustrates how climate-driven variation in flow influences environmental conditions and phytoplankton communities in the Coorong, a Ramsar-listed shallow coastal lagoon of international importance. We show that changes in salinity and water level, regulated by freshwater inputs, are the primary drivers of phytoplankton abundance, diversity and community composition. Secondary drivers included distance from the Murray Mouth and temperature, with pH and nutrient concentrations also significant in distance-based linear models and generalised additive models, though with weaker influence. Categorising phytoplankton communities by salinity-defined habitats provided a useful way to describe patterns along the Coorong's longitudinal salinity gradient. This habitat-based approach enables predictions of phytoplankton responses under future climate change scenarios where salinity projections are available. It also offers a transferable framework for other lagoon systems that experience wide salinity ranges and strong spatial and temporal variability.

6. References

Ahyong S, Boyko CB, Bernot J, Brandão SN, Daly M, De Grave S, de Voogd NJ, Gofas S, Hernandez F, Mees J, Neubauer TA, Paulay G, van der Meij S, Boydens B, Dekeyzer S, Goharimanesh M, Vandepitte L, Vanhoorne B, Agatha S, Zullini A (2026). World Register of Marine Species (WoRMS). www.marinespecies.org.

Aldridge KT, and Brookes JD (2011). *The response of water quality and phytoplankton communities in the Northern Lagoon of the Coorong and Murray Mouth to barrage releases from the Lower Lakes, November 2010 - May 2011*. Final report prepared for the Department of Environment and Natural Resources and Department for Water, the Government of South Australia, Adelaide, South Australia.

Alegria Zufia J, Farnelid H, and Legrand C (2021). Seasonality of coastal picophytoplankton growth, nutrient limitation, and biomass contribution. *Front Microbiol*, 12, 786590.

Anderson DM (2012). HABs in a changing world: a perspective on harmful algal blooms, their impacts, and research and management in a dynamic era of climactic and environmental change. *Harmful Algae*, 2012, 3–17.

Anderson DM, Alpermann TJ, Cembella AD, Collos Y, Masseret E, and Montresor M (2012). The globally distributed genus *Alexandrium*: multifaceted roles in marine ecosystems and impacts on human health. *Harmful Algae*, 14, 10–35.

Anderson MJ, and Willis TJ (2003). Canonical analysis of principal coordinates: a useful method of constrained ordination for ecology. *Ecology*, 84(2), 511–525.

Asanopoulos C, and Waycott M (2020). The growth of aquatic macrophytes (Ruppia tuberosa spp. and Althenia cylindrocarpa) and the filamentous algal community in the southern Coorong. University of Adelaide, Adelaide.

Baker ME, and King RS (2010). A new method for detecting and interpreting biodiversity and ecological community thresholds, *Methods in Ecology and Evolution,* 1, 25–37.

Bakker ES, and Hilt S (2015). Impact of water-level fluctuations on cyanobacterial blooms: options for management. *Aquatic Ecology*, 50(3), 485–498.

Balech E (1989). Redescription of Alexandrium minutum Halim (Dinophyceae) type species of the genus Alexandrium. *Phycologia*, 28, 206–211.

Balzano S, Ellis AV, Le Lan C, and Leterme SC (2015). Seasonal changes in phytoplankton on the north-eastern shelf of Kangaroo Island (South Australia) in 2012 and 2013. *Oceanologia*, 57(3), 251–262.

Barua A, Ajani PA, Ruvindy R, Farrell H, Zammit A, Brett S, Hill D, Sarowar C, Hoppenrath M, and Murray SA (2020). First detection of paralytic shellfish toxins from Alexandrium pacificum above the tegulatory limit in blue mussels (*Mytilus galloprovincialis*) in New South Wales, Australia. *Microorganisms*, 8(6), 905.

BOM (2025). Long-range weather and climate. The Australian Bureau of Meteorology Retrieved 20/10/2025 from https://www.bom.gov.au/location/australia/south-australia/upper-south-east/bsa_pt074-meningie

Bonacina L, Fasano F, Mezzanotte V, and Fornaroli R (2023). Effects of water temperature on freshwater macroinvertebrates: a systematic review. *Biological Reviews of The Cambridge Philosophical Society*, 98(1), 191–221.

Brookes JD, Aldridge KT, Bice CM, Deegan B, Ferguson GJ, Paton DC, Sheaves M, Ye Q, and Zampatti BP (2015). Fish productivity in the lower lakes and Coorong, Australia, during severe drought. *Transactions of the Royal Society of South Australia*, 139(2), 189–215.

Brookes JD, Busch B, Cassey P, Chilton D, Dittmann S, Dornan T, Giatas G, Gillanders BM, Hipsey M, Huang P, Keneally C, Jackson MV, Mosley L, Mott R, Paton D, Prowse T, Waycott M, Ye Q, Zhai S, and Gibbs M (2023). How well is the basin plan meeting its objectives? From the perspective of the Coorong, a sentinel of change in the Murray-Darling Basin. Australasian Journal of Water Resources, 27(2), 1–18.

Brookes JD, Huang P, Zhai SY, Gibbs MS, Ye Q, Aldridge KT, Busch B, and Hipsey, MR (2022). Environmental flows to estuaries and coastal lagoons shape the salinity gradient and generate suitable fish habitat: Predictions from the Coorong, Australia. *Frontiers in Environmental Science*, 10, 796623.

Burdick SM, Hewitt DA, Martin BA, Schenk L, and Rounds SA(2020). Effects of harmful algal blooms and associated water-quality on endangered Lost River and shortnose suckers. Harmful Algae, 97, 101847.

Callieri C, Modenutti B, Queimaliños C, Bertoni R, and Balseiro E (2007). Production and biomass of picophytoplankton and larger autotrophs in Andean ultraoligotrophic lakes: differences in light harvesting efficiency in deep layers. *Aquatic Ecology*, 41(4), 511–523.

Cardoso SJ, Roland F, Loverde-Oliveira SM, and de Moraes Huszar VL (2012). Phytoplankton abundance, biomass and diversity within and between Pantanal wetland habitats. *Limnologica*, 42(3), 235–241.

Chandel P, Mahajan D, Thakur K, Kumar R, Kumar S, Brar B, Sharma D, and Sharma, AK (2023). A review on plankton as a bioindicator: A promising tool for monitoring water quality. *World Water Policy*, 10(1), 213–232.

Chen D, Shi Z, Li R, Li X, Cheng Y, and Xu J (2023). Hydrodynamics drives shifts in phytoplankton community composition and carbon-to-chlorophyll a ratio in the northern South China Sea. *Frontiers in Marine Science*, 10, 1293354.

Chen T, and Guestrin C (2016). XGBoost: A scalable tree boosting system. *arXiv*,1603.02754v3.

Chilton D, Hamilton DP, Nagelkerken I, Cook P, Hipsey MR, Reid R, Sheaves M, Waltham NJ, and Brookes JD (2021). Environmental flow requirements of estuaries: Providing resilience to current and future climate and direct anthropogenic changes. *Frontiers in Environmental Science*, 9, 764218.

Cunha M, Nardi A, Botelho MJ, Sales S, Pereira E, Soares A, Regoli F, and Freitas R (2024). Can exposure to Gymnodinium catenatum toxic blooms influence the impacts induced by Neodymium in Mytilus galloprovincialis mussels? What doesn't kill can make them stronger? *Journal of Hazardous Materials*, 471, 134220.

da Costa MRA, Attayde JL, and Becker V (2015). Effects of water level reduction on the dynamics of phytoplankton functional groups in tropical semi-arid shallow lakes. *Hydrobiologia*, 778(1), 75–89.

de Wit R, Leruste A, Le Fur I, Sy MM, Bec B, Ouisse V, Derolez V, and Rey-Valette,H (2020). A multidisciplinary approach for restoration ecology of shallow coastal lagoons, a case study in South France. *Frontiers in Ecology and Evolution*, 8, 108.

Dang HV, Kermode S, Huang P, Carey CC, and Hipsey, MR (2025). Phytoplankton group classification by integrating trait information and observed environmental thresholds, Ecological Informatics, 90, 103212.

Death RG (2008). *Margalef's Index*. In SE Jørgensen and BD Fath (Eds.), Encyclopedia of Ecology. Elsevier B. V. Amsterdam, Netherlands.

Deng H, Shang X, Zhu H, Huang N, Wang L, and Sun M (2025). Saxitoxin: a comprehensive review of its history, structure, toxicology, biosynthesis, Detection, and preventive implications. *Marine Drugs*, 23(7), 277.

Deng Y, Xu X, Xu J, Wang W, Lu R, Zhuo H, Wang Y, Liu Y, Liu X, and Huang X (2024). Hydrological-driven changes in the phytoplankton community structure under nutrient stress in island river ecosystems. *Journal of Sea Research,* 202, 102548.

Derot J, Yajima H, and Jacquet S (2020). Advances in forecasting harmful algal blooms using machine learning models: a case study with Planktothrix rubescens in Lake Geneva. *Harmful Algae,* 99, 101906.

DEW (2025). Water Data SA. Department for Environment and Water, Adelaide. Retrieved 26/06/2025 from https://water.data.sa.gov.au/Data/Map/Parameter/NoParameter/Location/Type/Interval/Latest

Dittmann S, Baring R, Baggalley S, Cantin A, Earl J, Gannon R, Keuning J, Mayo A, Navong N, Nelson M, Noble W, and Ramsdale T (2015). Drought and flood effects on macrobenthic communities in the estuary of Australia's largest river system. *Estuarine, Coastal and Shelf Science*, 165, 36–51.

Dormann CF, Elith J, Bacher S, Buchmann C, Carl G, Carré G, Marquéz JRG, Gruber B, Lafourcade B, Leitão PJ, Münkemüller T, McClean C, Osborne PE, Reineking B, Schröder B, Skidmore AK, Zurell D, and Lautenbach S (2013). Collinearity: a review of methods to deal with it and a simulation study evaluating their performance. *Ecography*, 36(1), 27–46.

Elloumi J, Carrias J-F, Ayadi H, Sime-Ngando T, and Bouaïn A (2009) Communities structure of the planktonic halophiles in the solar saltern of Sfax, Tunisia. Estuarine, Coastal and Shelf Science, 81(1), 19–26.

Environmental Health Directorate (2022). *Environmental quality criteria for toxic algae in marine recreational water*. Government of Western Australia, Department of Health, East Perth.

Fairbridge RW (1980). *The estuary: its definition and geodynamic cycles*. In E Olausson and I Cato (Eds.), Chemistry and Geochemistry of Estuaries, John Wiley, New York, USA.

Flöder S, and Burns CW (2004). Phytoplankton diversity of shallow tidal lakes: influence of periodic salinity changes on diversity and species number of a natural assemblage. *Journal of Phycology*, 40(1), 54–61.

Flöder S, Jaschinski S, Wells G, and Burns CW (2010). Dominance and compensatory growth in phytoplankton communities under salinity stress. *Journal of Experimental Marine Biology and Ecology*, 395(1-2), 223–231.

Garcia-Oliva O, and Wirtz K (2025). The complex structure of aquatic food webs emerges from a few assembly rules. Nature Ecology and Evolution, 9(4), 576–588.

Garrido J, Perez-Bilbao A, and Benetti CJ (2011) *Biodiversity and conservation of coastal lagoons*. In O Grillo and G. Venora (Eds.), Ecosystems Biodiversity (pp. 12–39). InTech, Rikeka, Croatia.

Giatas G, Lamontagne S, Bice CM, Ye Q, and Paton DC (2018). *Food webs of the Coorong*. In LM Mosley, Q Ye, S Shepard, S Hemming, and PJ Fitzpatrick (Eds.), Natural History of the Coorong, Lower Lakes and Murray Mouth Region (Yarluwar-Ruwe) (pp. 422–441). University of Adelaide Press, Adelaide, Australia.

Hallegraeff GM, Bolck CJS, Hill RDA, Jameson I, LeRoi JM, McMinn A, Murray S, de Salas MF, and Saunders K (2010). *Algae of Australia: Phytoplankton of Temperate Coastal Waters*. CSIRO Publishing, Canberra, Australia.

Hallegraeff GM, McCausland MA, and Brown RK (1995). Early warning of toxic dinoflagellate blooms of Gymnodinium catenatum in southern Tasmanian waters. *Journal of Plankton Research*, 17(6), 1163–1176.

Hallegraef, GM, Schweibold L, Jaffrezic E, Rhodes L, MacKenzie L, Hay B, and Farrell H (2021) Overview of Australian and New Zealand harmful algal species occurrences and their societal impacts in the period 1985 to 2018, including a compilation of historic records. Harmful Algae, 102, 101848.

Hansen HP, and Koroleff F (1999). *Determination of nutrients*. In K Grasshoff, K Kremling, and M Ehrhardt (Eds.), Methods of Seawater Analysis (pp. 159–228). Wiley-VCH, Weinheim, Germany.

Hemming S, Rigney D, Rigney G, Trevorrow L, Muller SL, and Della-Sale A (2018). *Ngarrindjeri vision for the ecological character of the Coorong and Lower Lakes*. In LM Mosley, Q Ye, S Shepard, S Hemming, and PJ Fitzpatrick (Eds.), Natural History of the Coorong, Lower Lakes and Murray Mouth Region (Yarluwar-Ruwe). The University of Adelaide Press, Adelaide, Australia.

Hemraj DA, Hossain A, Ye Q, Qin JG, and Leterme SC (2017). Anthropogenic shift of planktonic food web structure in a coastal lagoon by freshwater flow regulation. *Scientific Reports,* 7, 44441.

Henson SA, Cael BB, Allen SR, and Dutkiewicz S (2021). Future phytoplankton diversity in a changing climate. *Nature Communincations*, 12(1), 5372.

Herrmann B, Cerbule K, Brčić J, Grimaldo E, Geoffroy M, Daase M, and Berge J (2022). Accounting for uncertainties in biodiversity estimations: a new methodology and *its application to the mesopelagic sound scattering layer of the High Arctic. Frontiers in Ecology and Evolution,* 10, 775759.

Hoagland P, Anderson DM, Kaoru Y, and White AW (2002). The economic effects of harmful algal blooms in the United States: estimates, assessment issues, and information needs. *Estuaries*, 25(4), 819–837.

Hort V, Abadie E, Arnich N, Bottein M-YD, and Amzil Z (2021). Chemodiversity of brevetoxins and other potentially toxic metabolites produced by Karenia spp. and Their metabolic products in marine organisms. *Marine Drugs*, 19(12), 656.

Hu Y, Si-Moussi S, and Thuiller W (2024). Introduction to deep learning methods for multi-species predictions. Methods in Ecology and Evolution, 16(1), 228–246.

Huang, P, Hennig, K, Kala, J, Andrys, J, Hipsey, MR (2020) Climate change overtakes coastal engineering as the dominant driver of hydrological change in a large shallow lagoon. *Hydrology and Earth System Sciences*, 24(11), 5673–5697.

Huang J, Welsh DT, Erler DV, Ferguson A, Brookes JD, Keneally C, Chilton D, Dittmann S, Lam-Gordillo O, Southgate M, Simpson S, and Mosley LM (2022). *Coorong nutrient cycling and fluxes*. Goyder Institute for Water Research, Adelaide, Australia.

Huang P, Mosley L, Brookes JD, Sims C, Waycott M, Paraska D, Zhai SY, and Hipsey MR (2024). Hydrologic versus biogeochemical control of nutrient dynamics in a shallow hypersaline coastal lagoon:iInsight from a coupled hydrodynamic-water quality model. *Journal of Geophysical Research: Biogeosciences,* 129(7), e2023JG007497.

Jamieson T, Chitsaz M, Waycott M, and Leterme SC (2022). *Microbial community composition of the southern Coorong including evaluating seasonal variation and sediment, water column, aquatic macrophytes and filamentous algae as substrates for microbial growth*. Goyder Institute for Water Research, Adelaide, South Australia.

Jendyk J, Hemraj DA, Brown MH, Ellis AV, and Leterme SC (2014). Environmental variability and phytoplankton dynamics in a South Australian inverse estuary. *Continental Shelf Research,* 91, 134–144.

Jeppesen E, Pierson D, and Jennings E (2021). Effect of extreme climate events on lake ecosystems. *Water,* 13(3).

Jöhnk KD, Huisman JEF, Sharples J, Sommeijer BEN, Visser PM, and Stroom JM (2008). Summer heatwaves promote blooms of harmful cyanobacteria. *Global Change Biology*, 14(3), 495–512.

Karpowicz M, Kornijów R, and Ejsmont-Karabin J (2023). Not a good place to live for most, but excellent for a few—diversity of zooplankton in a shallow coastal ecosystem. *Sustainability*, 15(3), 2345.

Keneally C, Chilton D, Dornan TN, Kidd SP, Gaget V, Toomes A, Lassaline C, Petrovski R, Wood L, and Brookes JD (2025). Multi-omics reveal microbial succession and metabolomic adaptations to flood in a hypersaline coastal lagoon. *Water Research*, 280, 123511.

Keneally C, Southgate M, Chilton D, Gaget V, Welsh DT, Mosley L, Erler DV, Kidd SP, and Brookes J (2024). Organic matter accumulation drives methylotrophic methanogenesis and microbial ecology in a hypersaline coastal lagoon. *Limnology and Oceanography*, 9999, 1–14.

Kim DH, Aldridge KT, Brookes JD, Ganf GG (2013). The effect of salinity on the germination of Ruppia tuberosa and Ruppia megacarpa and implications for the Coorong: A coastal lagoon of southern Australia. *Aquatic Botany*, 111, 81–88.

Kim DH, Aldridge KT, Ganf GG, and Brookes JD (2015). Physicochemical influences on Ruppia tuberosa abundance and distribution mediated through life cycle stages. *Inland Waters*, 5(4), 451–460.

Kingsford TR, Walker FK, Lester ER, Young JW, Fairweather GP, Sammut J, and Geddes CM (2011). A Ramsar wetland in crisis – the Coorong, Lower Lakes and Murray Mouth. Marine and Freshwater Research, 62, 255–265.

Kjerfve, B (1994) *Chapter 1 Coastal Lagoons*. In Coastal Lagoon Processes (pp. 1–8). https://doi.org/10.1016/s0422-9894(08)70006-0

Lai J, Tang J, Li T, Zhang A, and Mao L (2024). Evaluating the relative importance of predictors in Generalized Additive Models using the gam.hp R package. *Plant Diversity*, 46(4), 542–546.

Lakane CP, Adams JB, and Lemley DA (2025). Phytoplankton responses to reduced freshwater inflow and acid conditions in a Ramsar estuarine lake. *Marine Environmental Research*, 206, 107043.

Lam-Gordillo O, Huang J, Barcelo A, Kent J, Mosley LM, Welsh DT, Simpson SL, and Dittmann S (2022). Restoration of benthic macrofauna promotes biogeochemical remediation of hostile sediments; An in situ transplantation experiment in a eutrophic estuarine-hypersaline lagoon system. *Science of the Total Environment*, 833, 155201.

Lam-Gordillo O, Mosley LM, Simpson SL, Welsh DT, and Dittmann S (2022). Loss of benthic macrofauna functional traits correlates with changes in sediment biogeochemistry along an extreme salinity gradient in the Coorong lagoon, Australia. *Marine Pollution Bulletin*, 174, 113202.

Lancelot C, and Muylaert K (2011). *Trends in estuarine phytoplankton ecology*. In E Wolanski and D McLusky (Eds.), Treatise on Estuarine and Coastal Science (pp. 5-15). Academic Press, London, UK.

Larson CA, and Belovsky GE (2013) Salinity and nutrients influence species richness and evenness of phytoplankton communities in microcosm experiments from Great Salt Lake, Utah, USA. *Journal of Plankton Research*, 35(5), 1154–1166.

Le Fur I, De Wit R, Plus M, Oheix J, Derolez V, Simier M, Malet N, and Ouisse, V (2019). Re-oligotrophication trajectories of macrophyte assemblages in Mediterranean coastal lagoons based on 17-year time-series. *Marine Ecology Progress Series*, 608, 13–32.

Lee WY, and Kuhn, NL (2019). Multivariate approach for identifying environmental indicator species in estuarine systems . *Marine Ecology Progress Series*, 611, 19–29.

Leira M, and Cantonati M (2008). Effects of water-level fluctuations on lakes: an annotated bibliography. *Hydrobiologia*, 613(1), 171–184.

Lester RE, Fairweather PG, Webster IT, and Quin RA (2013). Scenarios involving future climate and water extraction: Ecosystem states in the estuary of Australia's largest river. *Ecological Applications*, 23(5), 984–998.

Leterme SC, Allais L, Jendyk J, Hemraj DA, Newton K, Mitchell J, and Shanafield M (2015). Drought conditions and recovery in the Coorong wetland, South Australia in 1997–2013. *Estuarine, Coastal and Shelf Science*, 163, 175–184.

Leterme SC, Prime E, Mitchell J, Brown MH, and Ellis AV (2013). Diatom adaptability to environmental change: a case study of two Cocconeis species from high-salinity areas. *Diatom Research*, 28(1), 29–35.

Li Z, Gao Y, Wang S, Lu Y, Sun K, Jia J, and Wang Y (2021). Phytoplankton community response to nutrients along lake salinity and altitude gradients on the Qinghai-Tibet Plateau. *Ecological Indicators*, 128, 107848.

Liu M, Huang Y, Hu J, He J, and Xiao X (2023). Algal community structure prediction by machine learning. *Environmental Science and Ecotechnology*, 14, 100233.

Londe LR, Novo EM, Barbosa C, and Araujo CA (2016). Water residence time affecting phytoplankton blooms: study case in Ibitinga Reservoir (Sao Paulo, Brazil) using Landsat/TM images. *Brazilian Journal of Biology*, 76(3), 664–672.

Loverde-Oliveira SM, Huszar VLM, Mazzeo N, and Scheffer M (2009). Hydrology-Driven Regime Shifts in a Shallow Tropical Lake. *Ecosystems*, 12(5), 807–819.

Lundberg M, and Lee, SI (2017). A unified approach to interpreting model predictions. *arXiv*, 1705.07874.

Lundholm N, Bernard C, Churro C, Escalera L, Hoppenrath M, Iwataki M, Larsen J, Mertens K, Murray S, Probert I, Salas R, Tillmann U, and Zingone A (2009 onwards). IOC-UNESCO Taxonomic Reference List of Harmful Microalgae. Retrieved 17-03-2026 from https://www.marinespecies.org/hab

Malinsky-Rushansky N, Berman T, Berner T, Yacobi YZ, and Dubinsky Z (2002). Physiological characteristics of picophytoplankton, isolated from Lake Kinneret: responses to light and temperature. *Journal of Plankton Research*, 24(11), 1173–1183.

Marie D, Partensky F, Jacquet S, and Vaulot D (1997). Enumeration and cell cycle analysis of natural populations of marine picoplankton by flow cytometry using the nucleic acid stain SYBR Green I. *Applied and Environmental Microbiology*, 63(1), 186–193.

Mayer M, and Standen A (2025). Package 'shapviz': SHAP visualizations. Version 0.10.3 R package.

McGrath GS, Huntley B, and Venarsky MP (2025). Variation of salinity with water level in shallow lakes is complex and rich in information. Journal of Hydrology, 660, 133347.

Mironova E, Telesh I, and Skarlato S (2013). Planktonic ciliates of the Neva Estuary (Baltic Sea): community structure and spatial distribution. *Acta Protozoologica*, 52(1), 13–23.

Mosley LM, Priestley S, Brookes JD, Dittmann S, Farkas J, Farrell M, Ferguson AJ, Gibbs M, Hipsey M, Huang J, Lam-Gordillo O, Simpson SL, Tyler JJ, Waycott M, and Welsh DT (2023). Extreme eutrophication and salinisation in the Coorong estuarine-lagoon ecosystem of Australia's largest river basin (Murray-Darling). *Marine Pollution Bulletin*, 188, 114648.

NHMRC (2008). *Guidelines for managing risks in recreational water*. National Health and Medical Research Council, Canberra, Australia.

Nicol J (2005). The ecology of *Ruppia* spp. in South Australia, with reference to the Coorong. SARDI Research Report Series No. 88, Adelaide, Australia.

Ogle DH, Doll JC, Wheeler AP, and Dinno A (2025). FSA: Simple fisheries stock assessment methods. Version 0.10.0 R package. https://CRAN.R-project.org/package=FSA.

Pan, Y, Guo, S, Li, Y, Yin, W, Qi, P, Shi, J, Hu, L, Li, B, Bi, S, Zhu, J (2018). Effects of water level increase on phytoplankton assemblages in a drinking water reservoir. Water, 10(3), 256.

Paton DC, Paton FL, and Bailey CP (2015). Ecological character description for Ruppia tuberosa in the Coorong. Univesity of Adelaide, Adelaide, Australia.

Paton DC, Rogers DJ, Aldridge K, Deegan B, and Brookes JD (2009a). A future for the Coorong and Lower Lakes. *Pacific Conservation Biology*, 15(1), 7–10.

Paton DC, Rogers DJ, Hill BM, Bailey CP, and Ziembicki M (2009b) Temporal changes to spatially stratified waterbird communities of the Coorong, South Australia: implications for the management of heterogenous wetlands. *Animal Conservation*, 12(5), 408–417.

Pedersen EJ, Miller DL, Simpson GL, and Ross N (2019). Hierarchical generalized additive models in ecology: an introduction with mgcv. *PeerJ*, 7, e6876.

Pedros-Alio C, Calderon-Paz JI, MacLean MH, Medina G, Marrase C, Gasol JM, Guixa-Boixereu N (2000). The microbial food web along salinity gradients. *FEMS Microbiology Ecology*, 32, 143–155.

Pinto A, Botelho MJ, Churro C, Asselman J, Pereira P, and Pereira JL (2023). A review on aquatic toxins - do we really know it all regarding the environmental risk posed by phytoplankton neurotoxins? *Journal of Environmental Management*, 345, 118769.

Priestley SC, Tyler J, Liebelt SR, Mosley LM, Wong WW, Shao Y, Woolston Z, Farrell M, Welsh DT, Brookes JD, Collins AS, Keneally C, and Farkaš J (2022). N and C isotope variations along an extreme eutrophication and salinity gradient in the Coorong Lagoon, South Australia. *Frontiers in Earth Science*, 9, 727971.

Priya AK, Muruganandam M, Rajamanickam S, Sivarethinamohan S, Gaddam MKR, Velusamy P, Gomathi R, Ravindiran G, Gurugubelli TR, and Muniasamy SK (2023). Impact of climate change and anthropogenic activities on aquatic ecosystem - a review. *Environmental Research*, 238, 117233.

R Core Team (2022). R: A Language and Environment for Statistical Computing. Version 4.2.0 R Foundation for Statistical Computing. https://www.R-project.org/

Rees G, Dunlop M, Grigg N, and Ahmad M (2022). *Trajectories of ecological change for the Coorong and Lower Lakes, in response to climate change*. Goyder Institute for Water Research, Adelaide, Australia.

Salmi P, Mäki A, Mikkonen A, Puupponen V-M, Vuorio K, and Tiirola M (2021). Comparison of epifluorescence microscopy and flow cytometry in counting freshwater picophytoplankton. *Boreal Environment Research*, 26, 17–27.

Schapira M, Buscot MJ, Pollet T, Leterme SC, and Seuront L (2010). Distribution of picophytoplankton communities from brackish to hypersaline waters in a South Australian coastal lagoon. *Saline Systems*, 6, 2.

Shapouri M, Cancela da Fonseca L, Iepure S, Stigter T, Ribeiro L, Silva A (2015). The variation of stygofauna along a gradient of salinization in a coastal aquifer. *Hydrology Research*, 47(1), 89–103.

Simpson GL (2024). gratia: An R package for exploring generalized additive models. *Journal of Open Source Software*, 9(104).

Singh S, Acharyya T, and Gopinath A (2022). *Phytoplankton ecology in Indian coastal lagoons: a review*. In S Madhav, S Nazneen, and P Singh (Eds.). Coastal Ecosystems, 38, 91–115.

Sitters V (2018). *European settlement across the end of the River Murray*. In L Mosley, Q Ye, S Shepherd, S Hemming, and R Fitzpatrick (Eds.), Natural History of the Coorong, Lower Lakes, and Murray Mouth region (Yarluwar-Ruwe). University of Adelaide Press. Adelaide, Australia.

Somogyi B, Felfoldi T, Boros E, Szabo A, and Voros L (2022). Where the little ones play the main role-picophytoplankton predominance in the soda and hypersaline lakes of the Carpathian Basin. *Microorganisms*, 10(4), 818.

Somogyi B, Voros L, Palffy K, Szekely G, Bartha C, and Keresztes ZG (2014). Picophytoplankton predominance in hypersaline lakes (Transylvanian Basin, Romania). *Extremophiles*, 18(6), 1075–1084.

Staudinger MD, Lynch AJ, Gaichas SK, Fox MG, Gibson-Reinemer D, Langan, JA, Teffer, AK, Thackeray SJ, and Winfield IJ (2021). How does climate change affect emergent properties of aquatic ecosystems? *Fisheries*, 46(9), 423–441.

Stein, ED, Gee, EM, Adams, JB, Irving, K, Van Niekerk, L (2021). Advancing the science of environmental flow management for protection of temporarily closed estuaries and coastal lagoons. *Water*, 13(5), 595.

Stewart, I, Schluter, PJ, and Shaw GR (2006). Cyanobacterial lipopolysaccharides and human health - a review. *Environmental Health*, 5(1), 7.

Sun X, Zhang H, Wang Z, Huang T, and Huang H (2022). Phytoplankton community response to environmental factors along a salinity gradient in a Seagoing River, Tianjin, China. *Microorganisms*, 11(1), 75.

Timbal B, Abbs D, Bhend J, Chiew F, Church J, Ekström M, Kirono D, Lenton A, Lucas C, McInnes K, Moise A, Monselesan D, Mpelasoka F, Webb L, and Whetton, P (2015). Murray Basin Cluster Report. In M Ekström, P Whetton, C Gerbing, MR Grose, L Webb, and JS Risbey (Eds.). *Climate Change in Australia: Projections for Australia's Natural Resource Management Regions*. CSIRO and Bureau of Meteorology. Canberra, Australia.

Timbal B, Fiddes S, and Brown JR (2017). Understanding south-east Australian rainfall projection uncertainties: the influence of patterns of projected tropical warming. *International Journal of Climatology,* 37(S1), 921–939.

Tunca H, Ongun Sevìndìk T, Ergül HA, Kaya M, Ekmekçì F, Kayal M, Güzel B, and Canli O (2024). The effects of salinity on phytoplankton community structure in the 6 lagoons of the Marmara Basin (Türkiye). *Biologia*, 79(5), 1251–1266.

Velasco J, Gutierrez-Canovas C, Botella-Cruz M, Sanchez-Fernandez D, Arribas P, Carbonell JA, Millan A, and Pallares S (2018). Effects of salinity changes on aquatic organisms in a multiple stressor context. *Philosophical Transactions of the Royal Society B*, 374(1764), 20180011.

Wang, Y, Fan, Z, Wang, W, Zhou, Z, Ye, X (2022). Effects of flood on phytoplankton diversity and community structure in Floodplain lakes connected to the Yangtze River. *Diversity*, 14(7), 581.

Webster IT (2010a). Dynamic assessment of oceanic connectivity in a coastal lagoon – the Coorong, Australia. *Journal of Coastal Research,* 27(1), 131–139.

Webster IT (2010b). The hydrodynamics and salinity regime of a coastal lagoon – the Coorong, Australia – seasonal to multi-decadal timescales. *Estuarine, Coastal and Shelf Science*, 90(4), 264–274.

Wells ML, Karlson B, Wulff A, Kudela R, Trick C, Asnaghi V, Berdalet E, Cochlan W, Davidson K, De Rijcke M, Dutkiewicz S, Hallegraeff G, Flynn KJ, Legrand C, Paerl H, Silke J, Suikkanen S, Thompson P, and Trainer VL (2020). Future HAB science: Directions and challenges in a changing climate. *Harmful Algae*, 91, 101632.

WHO (2022). *Guidelines for drinking-water quality: fourth edition incorporating the first and second addenda*. World Health Organisation, Geneva, Switzerland.

Winder M, and Sommer U (2012). Phytoplankton response to a changing climate. *Hydrobiologia*, 698(1), 5–16.

Wurtsbaugh WA, Paerl HW, and Dodds WK (2019). Nutrients, eutrophication and harmful algal blooms along the freshwater to marine continuum. *WIREs Water*, 6(5), e1373.

Xu Y, Zhang D, Lin J, Peng Q, Lei X, Jin T, Wang J, and Yuan R (2024). Prediction of phytoplankton biomass and identification of key influencing factors using interpretable machine learning models. *Ecological Indicators*, 158, 111320

Yang C, Shen X, Wu J, Shi X, Cui Z, Tao Y, Lu H, Li J, and Huang Q (2023). Driving forces and recovery potential of the macrophyte decline in East Taihu Lake. *Journal of Environmental Management*, 342, 118154.

Yvon-Durocher G, Allen AP, Montoya JM, Trimmer M, and Woodward G (2010). The temperature dependence of the carbon cycle in aquatic ecosystems. *Advances in Ecological Research*, 43, 267–313.

Zhang Q, Huang Y, and An S (2025). Quantification of phytoplankton groups using in-situ multi-excitation chlorophyll fluorescence measurements and machine learning (mf-ML). *Algal Research*, 90, 104155.

Zhang Z, Tang Q, Zhao G, Gaffney PPJ, and Dubois N (2024). Lake depth, a key parameter regulating evaporation in semi-arid regions: A case study from Dali Lake, China. *Hydrological Processes*, 38(6), e15196.


RESEARCH CENTRE
GOYDER
INSTITUTE
FOR WATER RESEARCH